

ANTENNA LABORATORY REPORT NO. 68-3

SOME ANALYTICAL METHODS FOR SOLVING A CLASS OF BOUNDARY VALUE PROBLEMS

AD 676300

by
G. F. VanBlaricum, Jr. and
R. Mitra

Contract No. AF19(628)-3219
Project No. 5635
Task No. 563502
Work Unit No. 56350201

Technical Report No. 15

JUNE 1968

Prepared for
AIR FORCE CAMBRIDGE RESEARCH LABORATORIES
OFFICE OF AEROSPACE RESEARCH
UNITED STATES AIR FORCE
BEDFORD, MASSACHUSETTS 01730
Contract Monitor - Robert A. Shore
Microwave Physics Laboratory

D D O
R
OCT 22 1968
REGISTRY
A



ANTENNA LABORATORY
DEPARTMENT OF ELECTRICAL ENGINEERING
UNIVERSITY OF ILLINOIS
URBANA, ILLINOIS 61801

DISTRIBUTION OF THIS DOCUMENT IS UNLIMITED

It may be released to the Clearinghouse,
Department of Commerce, for sale to the general public.

AFCRL-68-0352

Antenna Laboratory Report No. 58-3

SOME ANALYTICAL METHODS FOR SOLVING A
CLASS OF BOUNDARY VALUE PROBLEMS

by

G. F. VanBlaricum, Jr. and

R. Mittra

Contract No. AF19(628)-3819

Project No. 5635

Task No. 563502

Work Unit No. 56350201

Technical Report No. 16

June 1958

Prepared for

Air Force Cambridge Research Laboratories
Office of Aerospace Research
United States Air Force
Bedford, Massachusetts 01730
Contract Monitor - Robert A. Shore
Microwave Physics Laboratory

Antenna Laboratory
Department of Electrical Engineering
University of Illinois
Urbana, Illinois 61801

DISTRIBUTION OF THIS DOCUMENT IS UNLIMITED

It may be released to the Clearinghouse, Department of Commerce, for sale to the general public.

SOME ANALYTICAL METHODS FOR SOLVING A
CLASS OF BOUNDARY VALUE PROBLEMS

Glenn F. VanBlaricum, Jr. and R. Mittra
Antenna Laboratory
University of Illinois

A class of electromagnetic boundary value problems in which the geometry may be divided into two semi-infinite regions can be solved exactly by the Wiener-Hopf technique. Examples of such geometries, called basic Wiener-Hopf geometries, are a parallel-plate waveguide bifurcation and an infinite array of thin plates. Certain of these basic Wiener-Hopf problems can also be formulated in terms of infinite sets of linear equations which may be solved exactly by the conventional residue-calculus technique. In general, however, the problems admitting exact solution by either the Wiener-Hopf or conventional residue calculus techniques are restricted to certain highly idealized geometries.

A variety of boundary value problems, related to basic Wiener-Hopf geometries but of more practical interest, may be solved by a modification of the conventional residue-calculus technique, by the generalized scattering matrix technique, or by a combination of the two methods. Solution of a class of infinite sets of equations by the modified residue-calculus technique (MRCT) is based on construction of a meromorphic function $f(w)$ satisfying certain criteria determined by the form of the equations as well as an auxiliary requirement imposed by the edge condition. The solution is obtained by integrating certain functions related to $f(w)$ over contours in the complex w -plane.

A rapidly convergent numerical method for constructing $f(w)$ in the MRCT is presented. The MRCT solution is given in a form convenient for computation, not involving numerical integration or solution of large order matrix equations which are time consuming and potentially inaccurate from a computational standpoint. In addition, the MRCT automatically guarantees satisfaction of the edge condition and includes built-in tests on the convergence of the solution.

An additional group of modified Wiener-Hopf geometries in which modal expansions are possible are solved by a combination of the MRCT and the generalized scattering matrix procedure. A scattering matrix description, including both propagating and evanescent modes, for a modified Wiener-Hopf geometry is obtained in a convergent Neumann series form by considering the phenomenon of multiple reflections between junctions in a related auxiliary geometry. Each of the auxiliary junction problems is solved either by exact methods or by the MRCT.

The analytical methods described in this thesis are applicable to waveguide discontinuities, including steps, bifurcations, and diaphragms, in both rectangular and circular waveguides; to phased arrays of dielectric-filled waveguides with thick walls; to a variety of diffraction surfaces and gratings; and to many other modified Wiener-Hopf geometries. Numerical examples of discontinuity, array, and grating problems are included to illustrate the application of the methods.

TABLE OF CONTENTS

	Page
I. INTRODUCTION.....	1
II. ANALYTICAL METHODS.....	4
III. INHOMOGENEOUSLY-FILLED WAVEGUIDE BIFURCATION.....	22
IV. THICK-WALL PHASED ARRAY.....	59
V. DIFFRACTING SURFACES AND GRATINGS.....	83
VI. CONCLUSIONS.....	92
REFERENCES.....	94
VITA.....	96

LIST OF TABLES

Table		Page
3.1	Reflection Coefficient for Inhomogeneously-Filled Bifurcated Waveguide.....	47
3.2	Truncated Scattering Matrix S^{AA} for Waveguide Step Discontinuity.....	50
4.1	Reflection Coefficient vs. Scan Angle for Thin-Wall Phased Array ($a/\lambda = 0.6205$).....	75
4.2	Reflection Coefficient vs. Scan Angle for Thick-Wall Phased Array ($a/\lambda = 0.6205, c/a = 0.02$).....	76
4.3	Reflection Coefficient vs. Scan Angle for Thick-Wall Phased Array ($a/\lambda = 0.6205, c/a = 0.063$).....	77
4.4	Reflection Coefficient vs. Scan Angle for Thick-Wall Phased Array ($a/\lambda = 0.6205, c/a = 0.12$).....	78
5.1	Reflection Coefficient for Diffracting Surface ($a = 0.75\lambda, d = 0.5\lambda$).....	91

LIST OF FIGURES

Figure	Page
2.1 H-plane waveguide bifurcation.....	15
2.2 Singly-inhomogeneous waveguide bifurcation.....	17
2.3 Auxiliary geometry for singly-inhomogeneous bifurcation..	18
2.4 Multiple reflection diagram for waveguide bifurcation....	19
3.1 Inhomogeneously-filled waveguide bifurcation.....	23
3.2 Auxiliary geometry for inhomogeneously-filled bifur- cation.....	25
3.3 Waveguide step discontinuity.....	37
3.4 Magnetic-wall, electric-wall termination.....	40
3.5 Reflection coefficient for inhomogeneously-filled bifurcation ($\epsilon_b = 1.0$, $a = 0.75\lambda$).....	46
3.6 Reflection coefficient for inhomogeneously-filled bifurcation ($\epsilon_b = 3.0$, $a = 0.75\lambda$).....	48
3.7 Amplitude of aperture electric field ($a = 0.75\lambda$).....	51
3.8 Reflection coefficient for waveguide step discontinuity ($a = 0.75\lambda$).....	53
3.9 Waveguide inductive diaphragm.....	54
3.10 Reflection coefficient for waveguide diaphragm discon- tinuity.....	57
4.1 Phased array of open-end rectangular waveguides.....	60
4.2 Infinite array of thin parallel plates.....	63
4.3 Thin-wall array reflection coefficient.....	68
4.4 Infinite array of thick parallel plates.....	70
4.5 Auxiliary geometry for thick-wall array.....	71
4.5 Reflection coefficients for thick-wall phased array.....	72
4.7 Aperture field for thick-wall array.....	81

LIST OF FIGURES (cont.)

Figure		Page
5.1	Infinite periodic diffracting surface.....	84
5.2	Metallic modulated diffracting surface.....	87
5.3	Infinite grating of thin strips.....	89

I. INTRODUCTION

It is well known that a class of boundary value problems may be solved exactly by the Wiener-Hopf technique (Noble [1958]). One method used in the solution of such problems by the Wiener-Hopf technique is formulation in terms of a semi-infinite range integral equation of the form

$$\int_c^{\infty} \phi(u)K(v-u)du = \psi(v) \quad (1.1)$$

where $\phi(u)$ is the unknown function and the kernel function $K(v)$ and the inhomogeneous term $\psi(v)$ are known from the geometry and the excitation. The solution of integral equations of the type (1.1) is discussed in the classical paper by Wiener and Hopf [1931].

An alternative procedure, often referred to in the literature as Jones' method (see Noble [1958]), leads directly to a Fourier-transformed version of (1.1) in the general form

$$K(\alpha) A_+(\alpha) = \Psi(\alpha) + B_-(\alpha), \quad (1.2)$$

where α is the Fourier transform variable. Equation (1.2) has two unknowns, A_+ and B_- , analytic in the upper and lower half planes, respectively, of the complex α -plane with a common strip of overlap. $K(\alpha)$ and $\psi(\alpha)$ are known functions.

An entirely different method for formulation and solution has been applied to a number of problems solvable by the Wiener-Hopf technique. The alternative approach is based on expansion of fields in terms of

normal modes of the semi-infinite regions and matching the resultant expressions at the plane of the interface. Fourier analysis of these field expressions leads to an infinite set of simultaneous linear equations for the mode coefficients. The exact solution of these equations by a residue-calculus technique is discussed in Section II. An alternative method of solution by direct inversion has been found by Mittra [1963].

The Wiener-Hopf method and the residue-calculus technique are quite versatile, finding application in rather diverse areas of mathematical physics, e.g., acoustic and electromagnetic wave propagation, design of optimal filters, etc. Also, the Wiener-Hopf and residue calculus techniques are the only known methods for exact solution of a class of problems not conforming to separable coordinate systems. Nonetheless, the scope of these techniques is limited to idealized geometries satisfying certain strict requirements.

In recent years, there have been attempts toward extending Wiener-Hopf and residue-calculus techniques to a wider class of problems of more practical interest. These may be described as modified Wiener-Hopf geometries, since they can be related to a basic Wiener-Hopf geometry. Typical examples are diffraction by a thick half-plane, scattering at the junction of two cylindrical or parallel-plate waveguides of dissimilar transverse dimension, radiation from a dielectric loaded waveguide phased array, etc. In this thesis, some methods are presented for formulating and solving a class of problems of the modified Wiener-Hopf type.

A rapidly-convergent numerical method based upon an extension of the conventional residue-calculus technique is presented for the solution of a class of infinite sets of simultaneous linear equations. In this method, the need for numerical inversion of large matrix equations, such as those derived in an integral equation approach to these boundary value problems, is eliminated. In the present approach, the solution is obtained in the same form as generated by the conventional residue-calculus method, permitting rapid numerical calculation. In addition, the procedure guarantees satisfaction of the edge condition, which is a significant advantage over certain iterative techniques where it is difficult to advance a direct proof that the edge condition is indeed satisfied.

A class of related problems is solved by the generalized scattering matrix procedure (Mittra and Pace [1963]), in which the method of multiple reflection between junctions is extended to include some junctions which are not exactly solvable, but for which very accurate numerical solutions can be obtained by the modified residue calculus technique. For the sake of completeness, a brief description of the scattering matrix procedure is included in Section II. Applications to phased arrays as well as diffracting surfaces and gratings are made in Sections IV and V, illustrating that a combination of the modified residue-calculus method and scattering matrix techniques is useful for resolving a rather large variety of boundary value problems which may be identified as modifications of the basic Wiener-Hopf geometry.

II. ANALYTICAL METHODS

The analytical methods applied to the problems in this thesis are described in this section. The methods are applicable to a class of modified Wiener-Hopf type geometries in which the electromagnetic fields may be expanded in terms of a discrete set of modes. The eigenvalue spectrum associated with these problems is discrete by virtue of either restriction to closed regions or periodicity in open regions. In this event, the fields are completely described by the set of mode coefficients. The methods described here are used to obtain the required mode coefficients by a rapidly convergent numerical technique.

The Modified Residue-Calculus Technique

The modified residue-calculus technique (MRCT) recently introduced by Mitra, Lee, and VanBlaricum [1968], is a method for the approximate solution of a class of infinite sets of simultaneous linear equations, such as those generated by a mode matching procedure at a discontinuity in a waveguide. When the equations admit an exact solution, the MRCT gives that solution, but the approximate solutions to other problems is obtained without the need for numerical inversion of extremely large-order matrix equations.

The appropriate sets of equations have the general form

$$\sum_{n=1}^{\infty} A_n \left(\frac{1}{\alpha_n - \gamma_m} + \frac{\lambda_m}{\alpha_n + \gamma_m} \right) = \left(\frac{1}{\alpha_p + \gamma_m} + \frac{\lambda_m}{\alpha_p - \gamma_m} \right), \quad m = 1, 2, 3, \dots \quad (2.1)$$

where $\{\alpha_n\}$, $\{\gamma_n\}$, $\{\lambda_n\}$ are all known and $\{A_n\}$ are to be determined. The MRCT is an extension of the conventional residue-calculus technique, which

provides an exact solution to a set of equations of the general form (2.1) when $\lambda_m = 0$, $m = 1, 2, 3, \dots$

The conventional residue-calculus technique was introduced by Berz [1951] and applied to the set of equations occurring in the problem of diffraction of a plane wave by a set of parallel plates. Subsequent applications of the technique have been made by Whitehead [1951], Hurd and Gruenberg [1954], and Wu and Galindo [1966] to cases which are relevant to certain aspects of this thesis. Another application of the method is found in Collin [1960].

The conventional residue-calculus technique can perhaps best be described by an example which is related to a set of equations derived in Section III. These equations, related to a simple waveguide bifurcation, are

$$\sum_{n=1}^{\infty} A_n \left(\frac{1}{\alpha_n - \beta_m} \right) = \frac{1}{\alpha_p + \beta_m}, \quad m = 1, 2, 3, \dots \quad (2.2)$$

$$\sum_{n=1}^{\infty} A_n \left(\frac{1}{\alpha_n - \gamma_m} \right) = \frac{1}{\alpha_p + \gamma_m}, \quad m = 1, 2, 3, \dots \quad (2.3)$$

where

$$\alpha_n = \sqrt{k_0^2 - (n\pi/a)^2} = -j \sqrt{(n\pi/a)^2 - k_0^2}$$

$$\beta_n = \sqrt{k_0^2 - (n\pi/b)^2} = -j \sqrt{(n\pi/b)^2 - k_0^2}$$

$$\gamma_n = \sqrt{k_0^2 - (n\pi/c)^2} = -j \sqrt{(n\pi/c)^2 - k_0^2}$$

and the equations are to be satisfied simultaneously.

It is desired to construct, by means of contour integrals of a known meromorphic function, equations of exactly the same form as (2.2)

and (2.3) and to solve for the $\{A_n\}$ by identifying corresponding terms.

The required meromorphic function $g(w)$ satisfies:

$$(g:1) \quad g(w) \text{ has simple poles at } w = \bar{\alpha}_1, \bar{\alpha}_2, \bar{\alpha}_3, \dots, \text{ and at } w = -\alpha_p.$$

$$(g:2) \quad g(\beta_n) = 0, \quad n = 1, 2, 3, \dots$$

$$(g:3) \quad g(\gamma_n) = 0, \quad n = 1, 2, 3, \dots$$

$$(g:4) \quad g(w) \text{ is algebraic (specifically } g(w) \sim Kw^{-3/2} \text{) as } |w| \rightarrow \infty$$

Condition (g:4) is a physical constraint of the problem (in this case, an edge condition) and insures a unique solution. Techniques for constructing such a function are well known, and $g(w)$ takes the form

$$g(w) = K \exp(Lw) \frac{\Pi(w, \beta) \Pi(w, \gamma)}{(w + \alpha_p) \Pi(w, \alpha)} \quad (2.4)$$

where

$$\Pi(w, \beta) = \prod_{n=1}^{\infty} \left(1 - \frac{w}{\beta_n}\right) \exp(jwb/n\pi) \quad (2.5)$$

and similarly for $\Pi(w, \alpha)$ with b replaced by a and $\Pi(w, \gamma)$ with b replaced by c . Also,

$$L = j \frac{a}{\pi} [\ln(a/b) + \frac{c}{a} \ln(b/c)] \quad (2.6)$$

In the complex w -plane, let C be a circle of infinite radius enclosing all of the poles and zeros of $g(w)$, and consider contour integrals of the type

$$\frac{1}{2\pi j} \oint \frac{g(w)}{w - \beta_m} dw, \quad m = 1, 2, 3, \dots,$$

and

$$\frac{1}{2\pi j} \int \frac{g(w)}{w-\gamma_m} dw, \quad m = 1, 2, 3, \dots$$

Applying the residue theorem and noting the properties of $g(w)$ stated above, one obtains the following identities:

$$\sum_{n=1}^{\infty} R_g(\alpha_n) \left(\frac{1}{\alpha_n - \beta_m} \right) - R_g(-\alpha_p) \left(\frac{1}{\alpha_p + \beta_m} \right) + g(\beta_m) = 0 \quad (2.7)$$

$$\sum_{n=1}^{\infty} R_g(\alpha_n) \left(\frac{1}{\alpha_n - \gamma_m} \right) - R_g(-\alpha_p) \left(\frac{1}{\alpha_p + \gamma_m} \right) + g(\gamma_m) = 0 \quad (2.8)$$

where $R_g(\alpha_n)$ = residue of $g(w)$ at $w = \alpha_n$. If $g(w)$ is normalized to make $R_g(-\alpha_p) = 1$, i.e.,

$$K = \frac{\exp(L\alpha_p) \Pi(-\alpha_p, \alpha)}{\Pi(-\alpha_p, \beta) \Pi(-\alpha_p, \gamma)}, \quad (2.9)$$

(2.7) and (2.8) may be identified with (2.2) and (2.3) and the solution given simply by

$$A_n = R_g(\alpha_n), \quad n = 1, 2, 3, \dots \quad (2.10)$$

The modified residue-calculus technique proceeds in a similar manner. Again, application to an example provides the most convenient exposition of the method. Suppose that the following equations are to be solved simultaneously:

$$\sum_{n=1}^{\infty} A_n \left(\frac{1}{\alpha_n - \gamma_m} + \frac{\lambda_m}{\alpha_n + \gamma_m} \right) = \frac{1}{\alpha_p + \gamma_m} + \frac{\lambda_m}{\alpha_p - \gamma_m} \quad (2.11)$$

$$\sum_{n=1}^{\infty} A_n \left(\frac{1}{\alpha_n - \beta_m} \right) = \frac{1}{\alpha_p + \beta_m} \quad (2.12)$$

As before, construct a meromorphic function $f(w)$ having specified properties:

- (f:1) $f(w)$ has simple poles at $w = \alpha_1, \alpha_2, \alpha_3, \dots$, and at $w = -\alpha_p$.
- (f:2) $f(\beta_n) = 0, n = 1, 2, 3, \dots$
- (f:3) $f(\gamma_n) + \lambda_n f(-\gamma_n) = 0, n = 1, 2, 3, \dots$
- (f:4) $f(w)$ is algebraic as $|w| \rightarrow \infty$. Specifically, $f(w) \sim Kw^{-\nu}$, $1 < \nu$, and the exact value of ν is determined by a physical constraint. It will be shown later that ν may be determined directly from the asymptotic behavior of the λ_m 's as m becomes large.

It will be noted that conditions (f:1) and (f:2) are identical to (g:1) and (g:2) imposed on $g(w)$, the function appropriate for the reduced problem with $\lambda_m \equiv 0$. Condition (f:3) is a generalization of (g:3).

If such a function $f(w)$ satisfying (f:1-4) can be constructed, then the solution to the equations proceeds as before. Consider the contour integrals along C

$$\frac{1}{2\pi j} \oint_C \left[\frac{f(w)}{w-\gamma_m} + \lambda_m \frac{f(w)}{w+\gamma_m} \right] dw, \quad m = 1, 2, 3, \dots,$$

and

$$\frac{1}{2\pi j} \oint_C \frac{f(w)}{w-\beta_m} dw, \quad m = 1, 2, 3, \dots$$

Again by residue techniques, the following results obtain:

$$\sum_{n=1}^{\infty} R_f(\alpha_n) \left(\frac{1}{\alpha_n - \gamma_m} + \frac{\lambda_m}{\alpha_n + \gamma_m} \right) - R_f(-\alpha_p) \left(\frac{1}{\alpha_p + \gamma_m} + \frac{\lambda_m}{\alpha_p - \gamma_m} \right) + [f(\gamma_m) + \lambda_m f(-\gamma_m)] = 0, m = 1, 2, 3, \dots \quad (2.13)$$

$$\sum_{n=1}^{\infty} R_f(\alpha_n) \left(\frac{1}{\alpha_n - \beta_m} \right) - R_f(-\alpha_p) \left(\frac{1}{\alpha_p + \beta_m} \right) + f(\beta_m) = 0, m = 1, 2, 3, \dots, \quad (2.14)$$

where $R_f(\alpha_n)$ = residue of $f(w)$ at $w = \alpha_n$. Provided $f(w)$ is normalized to make $R_f(-\alpha_p) = 1$, (2.13) and (2.14) may be identified with (2.11) and (2.12) yielding

$$A_n = R_f(\alpha_n), n = 1, 2, 3, \dots \quad (2.15)$$

Construction of $f(w)$. The key step in the modified residue-calculus technique is the construction of $f(w)$. Unlike in the conventional technique where all of the poles and zeros of the function as well as its asymptotic behavior are prescribed, in the modified technique only a subset of the collection of zeros is known explicitly, while all of the poles and the asymptotic behavior are again known. Since $f(w)$ must coincide with $g(w)$ in the limiting case $\lambda_m \equiv 0$, $f(w)$ may be written in the following form:

$$f(w) = K' \exp(Lw) \frac{\Pi(w, \beta) \Pi(w, \gamma')}{(w + \alpha_p) \Pi(w, \alpha)}, \quad (2.16)$$

where L , $\Pi(w, \beta)$, and $\Pi(w, \alpha)$ are given by (2.5) and (2.6), and where

$$\Pi(w, \gamma') = \prod_{n=1}^{\infty} \left(1 - \frac{w}{\gamma_n'} \right) \exp(+jw c / n\pi), \quad (2.17)$$

with $\{\gamma_n'\}$ being the as yet unknown zeros of $f(w)$. Comparison of $f(w)$ with $g(w)$ shows that except for constant factors the two functions are related by shifting an infinite set of zeros $\{\gamma_n\}$ of $g(w)$ to $\{\gamma_n'\}$ of $f(w)$, and that when $\lambda_m \equiv 0$, the zeros must coincide.

The asymptotic values of the set $\{\gamma_n'\}$ may be determined by imposing condition (f:3). Let $D_n = \gamma_n' - \gamma_n$ be the difference of the zeros. Condition (f:3) requires:

$$K' \exp(L\gamma_m) \frac{\prod(\gamma_m, \beta) \prod(\gamma_m, \gamma')}{(\gamma_m + \alpha_p) \prod(\gamma_m, \alpha)} + \lambda_m \frac{K' \exp(-L\gamma_m) \prod(-\gamma_m, \beta) \prod(-\gamma_m, \gamma')}{(-\gamma_m + \alpha_p) \prod(-\gamma_m, \alpha)} = 0, m = 1, 2, 3, \dots \quad (2.18)$$

For m large, the constants may be replaced by their asymptotic values, i.e., $\beta_n \sim -jn\pi/b$, $\alpha_n \sim -jn\pi/a$, $\gamma_n \sim -jn\pi/c$, and $D_n \sim D$ (an assumed asymptotic value), so that (2.18) becomes approximately

$$K' \exp(-jL\frac{m\pi}{c}) \frac{\prod_{n=1}^{\infty} [(1 - \frac{mc}{nb}) \exp(\frac{mc}{nb})]}{(-j\frac{n\pi}{c} + \alpha_p) \prod_{n=1}^{\infty} [(1 - \frac{mc}{na}) \exp(\frac{mc}{na})]} \frac{\prod_{n=1}^{\infty} [(1 - \frac{m}{n+jDc/\pi}) \exp(\frac{m}{n})]}{[(1 + \frac{m}{n+jDc/\pi}) \exp(-\frac{m}{n})]} + \lambda_m K' \exp(+jL\frac{m\pi}{c}) \frac{\prod_{n=1}^{\infty} [(1 + \frac{mc}{nb}) \exp(-\frac{mc}{nb})]}{(+j\frac{n\pi}{c} + \alpha_p) \prod_{n=1}^{\infty} [(1 + \frac{mc}{na}) \exp(-\frac{mc}{na})]} \frac{\prod_{n=1}^{\infty} [(1 + \frac{m}{n+jDc/\pi}) \exp(-\frac{m}{n})]}{[(1 + \frac{m}{n+jDc/\pi}) \exp(-\frac{m}{n})]} = 0, m = 1, 2, 3, \dots \quad (2.19)$$

Equation (2.19) can be reduced by observing that the infinite products take the form of an infinite product expansion for the gamma function (see Noble [1958]).

$$\prod_{n=1}^{\infty} \left(1 + \frac{x}{an+b}\right) \exp(-x/an)$$

$$= \begin{cases} \exp(-cx/a) \frac{\Gamma(1+b/a)}{\Gamma(1+b/a + x/a)} \\ \text{for } x \neq -|x| \end{cases} \quad (2.20a)$$

$$2 \sin(-x\pi/a - b\pi/a) \frac{\exp(-Cx/a) \Gamma(1+b/a)}{\Gamma(1+b/a - x/a)}$$

$$\text{for } x = -|x| \quad (2.20b)$$

where $C = \text{Euler's constant}$.

Utilizing these relations in (2.19), one has after rearranging and canceling like terms:

$$2 \sin(-m\pi - jcD) = + \lambda_m \sin(-m\pi a/c) / \sin(-m\pi b/c) \quad (2.21)$$

But $\sin(-m\pi a/c) = \sin(-m\pi - m\pi b/c) = (-1)^m \sin(-m\pi b/c)$

and $\sin(-m\pi - jcD) = (-1)^{m+1} \sin(jcD)$, so that (2.21) becomes, in the limit as $m \rightarrow \infty$,

$$2 \sin(jcD) = - \lim_{m \rightarrow \infty} \lambda_m$$

or
$$D = \frac{1}{jc} \sin^{-1} \left(- \frac{1}{2} \lim_{m \rightarrow \infty} \lambda_m \right) \quad (2.22)$$

The explicit evaluation of $D = \lim_{n \rightarrow \infty} D_n$ permits *a priori* determination of how the zeros of $f(w)$ are to be shifted for large indices. It will be shown subsequently that an expression equivalent to (2.22) may be obtained directly from the edge condition.

Exact determination of the shifted zeros $\{\gamma_n'\}$ for every n is not possible. However, for purposes of numerical computation it suffices to use the determined asymptotic value for all but the first few, say M of them, and to find those first M values explicitly. Also, except for exponential factors and an irrelevant constant factor K'' , the first M terms of the infinite product may in general be replaced by a polynomial of degree M . That is,

$$K'' \prod_{n=1}^M (1-w/\gamma_n') = w^M + a_1 w^{M-1} + \dots + a_{M-1} w + a_M$$

$$= P(w) \tag{2.23}$$

where to specify the functional behavior it is sufficient to determine the M polynomial coefficients a_1, a_2, \dots, a_M .

Accordingly, the function may be written

$$f(w) = K' P(w) \frac{\exp(Lw) \Pi(w, \beta) \Pi^{(M)}(w, \gamma')}{(w + \alpha_p) \Pi(w, \alpha)} \tag{2.24}$$

where $\Pi^{(M)}(w, \gamma')$ denotes the omission of the first M factors from (2.17) and replacement of γ_n' by $\gamma_n + D$ for all $n > M$. For simplification write

$$f(w) = K' P(w) f'(w), \tag{2.25}$$

where $f'(w)$ incorporates all of the known parts of $f(w)$.

The polynomial coefficients may be determined by imposing condition (f:3) for $n = 1, 2, 3, \dots, M$. Specifically,

$$K' [\gamma_n^M + a_1 \gamma_n^{M-1} + \dots + a_{M-1} \gamma_n + a_M] f'(\gamma_n)$$

$$+ \lambda_n K' [(-\gamma_n)^M + a_1(-\gamma_n)^{M-1} + \dots + a_{M-1}(-\gamma_n) + a_M] f'(-\gamma_n) = 0$$

for $n = 1, 2, 3, \dots, M, \quad (2.26)$

yielding a set of M simultaneous linear equations for a_1, a_2, \dots, a_M . Solution of the set of equations may be accomplished by usual numerical methods. Once $P(w)$ is known, the constant K' may be chosen to satisfy $R_F(-\alpha_p) = 1$.

It must be noted, however, that even though the MRCT requires numerical solution of a set of linear equations, the difficulty of that solution in no way approaches that of attempting a direct inversion of a truncated form of the original infinite set. For most instances, it suffices to solve a 5×5 or smaller set of equations explicitly in the MRCT, while much larger ones would be appropriate for the truncated set. In addition, the truncated set for (2.11) and (2.12) is quite ill-conditioned, while the set for the MRCT is well-behaved. An example in Section III illustrates the rapid convergence of the solution via the MRCT for a waveguide step discontinuity.

An additional feature of the MRCT for numerical work is that a built-in convergence test is available, because the function found numerically must satisfy conditions (f:2) and (f:3). A numerical test of these conditions may be almost trivially incorporated into a computer program.

Perhaps the greatest advantage of the MRCT is that satisfaction of the edge-condition via (f:4) is *a priori* guaranteed. And, more importantly, when the slight modifications of the geometry alter the edge behavior, the correction is made automatically in the MRCT. A further discussion of this property is given in Section III.

Generalized Scattering Matrix Technique

The generalized scattering matrix technique is another method for solving a class of boundary value problems. The concept of a generalized scattering matrix, introduced by Mittra and Pace [1963] is very closely related to the scattering matrix of circuit theory (Seshu and Balabanian [1959]) or of microwave network theory (Collin [1966]). However, it differs in that it is extended to consider evanescent as well as propagating modes, so that in waveguide junction problems, the scattering matrix will in general be of infinite order. (In subsequent discussions, the term "scattering matrix" will mean "generalized scattering matrix.")

The scattering matrix is defined for a junction between two regions in which the fields may be expanded in modes, such as the waveguide bifurcation of Figure 2.1. If the n^{th} TE mode is incident upon the plane $z=0$ from region (A), fields are reflected back into (A) and transmitted into (B) and (C). The E_y component of the field is expanded in a Fourier sine series, and the coefficient of the n^{th} mode referred to the plane $z=0$ is defined as the amplitude of that mode. If the amplitude of the n^{th} mode incident in (A) is one, then the amplitude of the m^{th} scattered mode in (A) is $S^{AA}(m,n)$ and the amplitude of the m^{th} transmitted mode in (B) is $S^{BA}(m,n)$. Terms $S^{AA}(m,n)$ and $S^{BA}(m,n)$ are the general matrix elements of S^{AA} and S^{BA} , respectively. The other scattering matrices are similarly defined.

In conventional scattering matrix formulations, the modes are normalized so that a propagating mode carries unit power. Since the generalized scattering matrix includes evanescent modes, such a

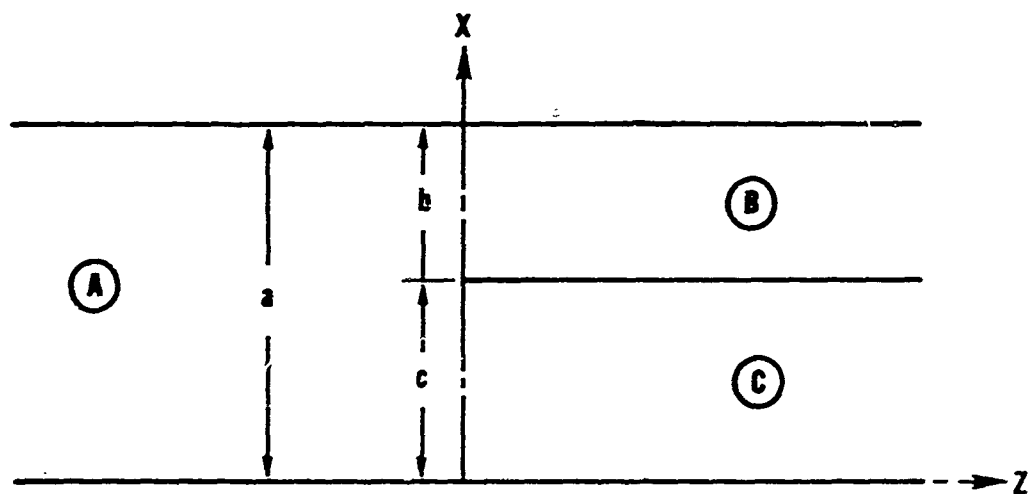


Figure 2.1 H-plane waveguide bifurcation

normalization is inappropriate. One consequence is that the scattering matrices are not symmetric.

The generalized scattering matrix technique is a means of solution for problems which are related to an exactly solvable auxiliary problem. For example, the inhomogeneously-filled waveguide bifurcation of Figure 2.2 is related to the simple bifurcation of Figure 2.1, which may be solved exactly by either Wiener-Hopf or residue-calculus techniques (Section III). If the dielectric region (C') is recessed as in Figure 2.3, the resultant problem involves two junctions, namely junction 1, the original bifurcation, and junction 2, the interface between regions (C) and (C'). Each junction problem may be solved individually and represented by scattering matrices, e.g. S_1^{AC} , S_1^{AB} , S_1^{CA} , S_1^{CC} , $S_2^{CC'}$, etc.

Suppose now that a TE wave is incident upon junction 1 from region (A). This wave is completely determined by the coefficients of the modes, and hence can be represented by a mode column vector ϕ such that ϕ_i is the coefficient of the i^{th} mode in the incident field. At junction 1, fields are reflected back into region (A) and transmitted into regions (B) and (C). The mode vector for the field reflected back into (A) is $S_1^{AA} \phi$, and for the field transmitted into (C), the vector is $S_1^{CA} \phi$. Part of the wave transmitted into (C) is reflected back into (C) and part is transmitted into (C') at junction 2. The mode vector in region (C') is $S_2^{C'C} S_1^{CA} \phi$. Figure 2.4 depicts symbolically the multiple reflection phenomena between junctions 1 and 2. The fields in each region are the sums of the fields transmitted or reflected successively. It should be noted, though,

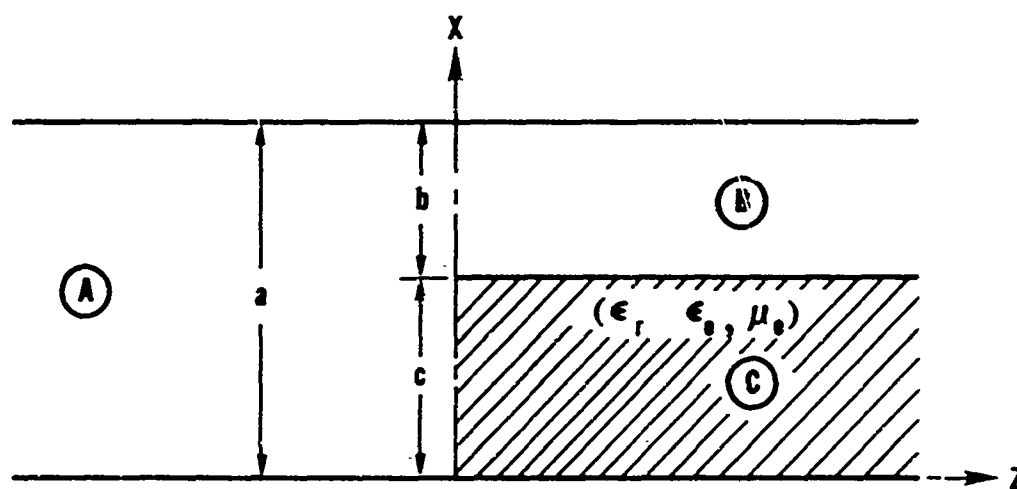


Figure 2.2 Singly-inhomogeneous waveguide bifurcation

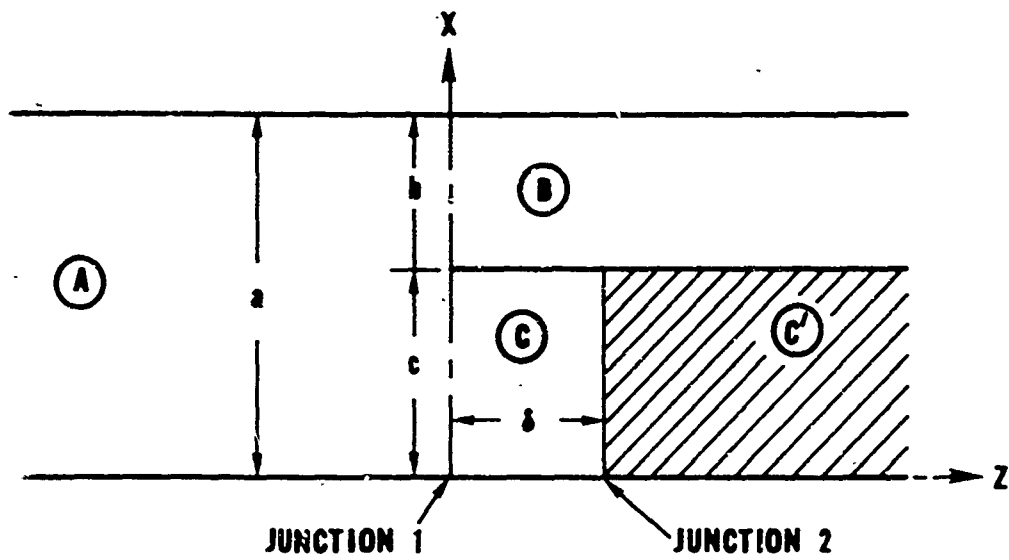


Figure 2.3 Auxiliary geometry for singly-inhomogeneous bifurcation

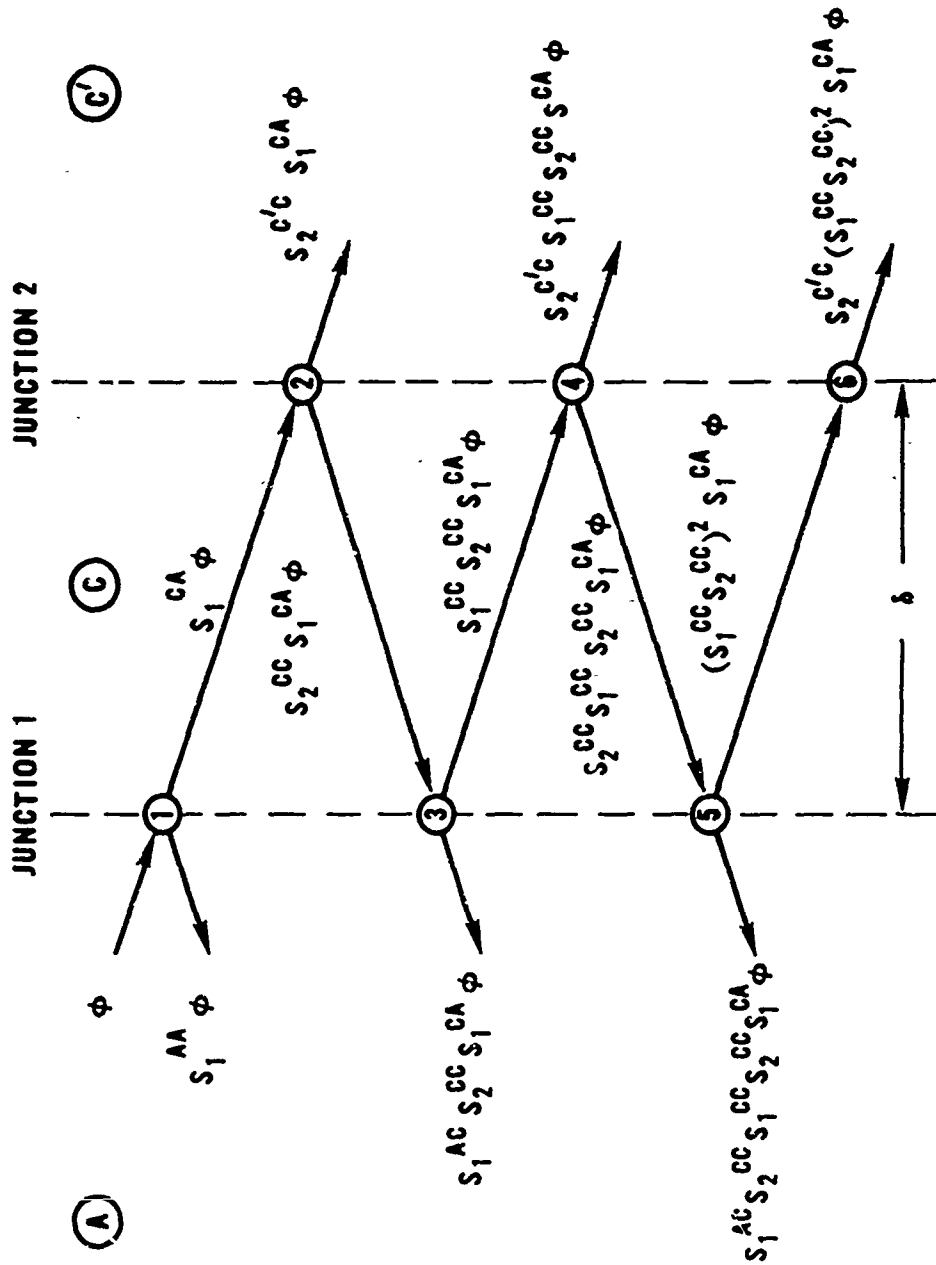


Figure 2.4 Multiple reflection diagram for waveguide bifurcation

that since the effect of propagation over the distance δ has been neglected, the results are valid only as $\delta \rightarrow 0$, in which case the geometry reduces to that of Figure 2.2, the desired geometry. The fields in the dielectric region may be represented by the mode vector ψ , which is found by summing the fields transmitted into (C').

$$\begin{aligned} \psi &= S_2^{C'C} S_1^{CA} \phi + S_2^{C'C} S_1^{CC} S_2^{CC} S_1^{CA} \phi \\ &+ S_2^{C'C} (S_1^{CC} S_2^{CC})^2 S_1^{CA} \phi + \dots \\ &= \sum_{n=0}^{\infty} S_2^{C'C} (S_1^{CC} S_2^{CC})^n S_1^{CA} \phi \end{aligned} \quad (2.27)$$

Equation (2.27) takes the form of a Neumann series, which can be summed in the standard way. Proof of the convergence is given in Pace [1964]. Also, the mode vector ψ must be given in terms of the composite junction scattering matrix (no subscript), so that

$$\begin{aligned} \psi &= S^{C'A} \phi \\ &= S_2^{C'C} (I - S_1^{CC} S_2^{CC})^{-1} S_1^{CA} \phi \end{aligned} \quad (2.28)$$

where I is the identity matrix. Since the result (2.28) is valid for arbitrary incident mode vector ϕ , the implication is that

$$S^{C'A} = S_2^{C'C} (I - S_1^{CC} S_2^{CC})^{-1} S_1^{CA} \quad (2.29)$$

The other scattering matrices for the problem can be found in an analogous manner.

Equation (2.29) is formally exact, since all of the auxiliary scattering matrices may be found exactly. For practical purposes, however, results are found approximately by truncating the scattering matrices and performing the inversion numerically. Many interesting problems may be solved approximately by the generalized scattering matrix procedure even when the auxiliary problem cannot be solved exactly. Often a very good approximate scattering matrix representation of the auxiliary problem can be found (for example, by the modified residue-calculus technique) so that the composite scattering matrices may be found as before. An example of this kind is given in Section III.

III. INHOMOGENEOUSLY-FILLED WAVEGUIDE BIFURCATION

Among the problems occurring in microwave theory are waveguide discontinuity problems. Most of the problems of interest do not possess exact solutions, so that many approximation techniques for the solution of such problems have been developed. Many such techniques and their application to finding equivalent transmission line and lumped circuit element representations for waveguide discontinuities are given by Marcuvitz [1951]. Since usually the equivalences are treated with respect to one or two propagating modes, description of discontinuities is often given in terms of modal reflection and transmission coefficients (i.e., scattering matrix elements).

The simple bifurcation problem (Figure 2.1) admits an exact solution, but the generalization to the inhomogeneously-filled bifurcation (Figure 3.1), which may be applied to waveguide junctions, waveguide diaphragms, and even to phased arrays, cannot be solved analytically in closed form. However, the modified residue calculus technique is expressly suited for solving such problems approximately and will be applied in this section to the solution of the inhomogeneously-filled waveguide bifurcation. Numerical results for a set of special cases are given, and application to related problems are discussed. Application of the results to the phased array is made in Section IV.

Analysis

The geometry of the inhomogeneously-filled bifurcation is given in Figure 3.1. The septum at $x = c$, $z \geq 0$, is assumed to be infinitely

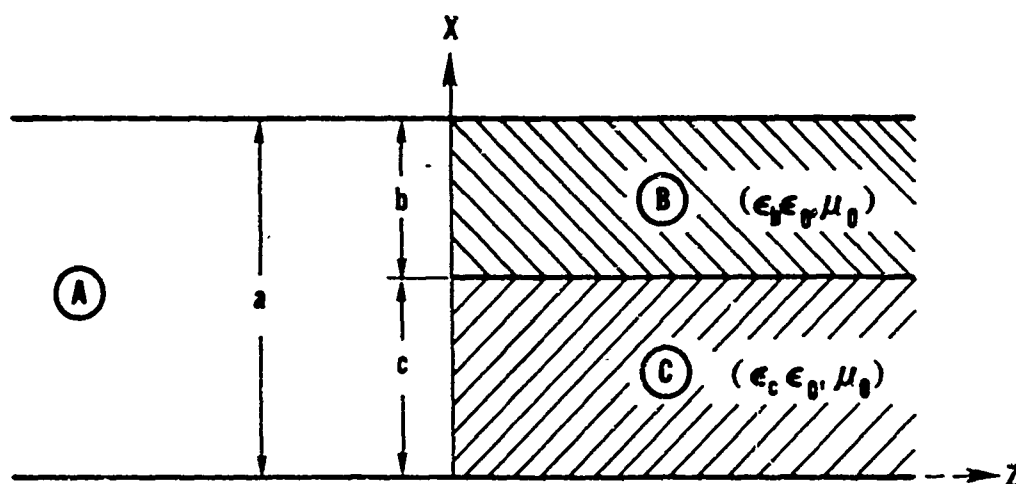


Figure 3.1 Inhomogeneously-filled waveguide bifurcation

thin and perfectly conducting. Regions (B) and (C) are filled with media of relative dielectric constants ϵ_b and ϵ_c , respectively. Assume that TE_{po} modes with electric vector parallel to the edge of the septum are incident upon the plane $z=0$ from regions (A) and (B) with amplitudes A and B, respectively. By linearity, the excitations may be treated either together or separately. No loss of generality results from not considering explicitly excitation from (C), since the role of (B) and (C) may be interchanged and the principle of superposition applied.

The total electromagnetic fields may be derived from the only non-zero component of electric field, E_y .

$$H_x = \frac{1}{j\omega\mu_0} \frac{\partial}{\partial z} (E_y) \quad (3.1a)$$

$$H_z = -\frac{1}{j\omega\mu_0} \frac{\partial}{\partial x} (E_y) \quad (3.1b)$$

($\exp(j\omega t)$ time variation is assumed throughout). The analysis and exact solution for the reduced problem $\epsilon_b = \epsilon_c = 1$ was given by Hurd and Gruenberg [1954]. Formulation for the generalized problem proceeds in a similar manner.

The formulation of the problem is facilitated by an auxiliary geometry, that of Figure 3.2. Dielectrics in regions (B) and (C) are recessed small distances u and v , forming regions (B') and (B''), and (C') and (C''), respectively. In the five regions, the transverse electric field may be written

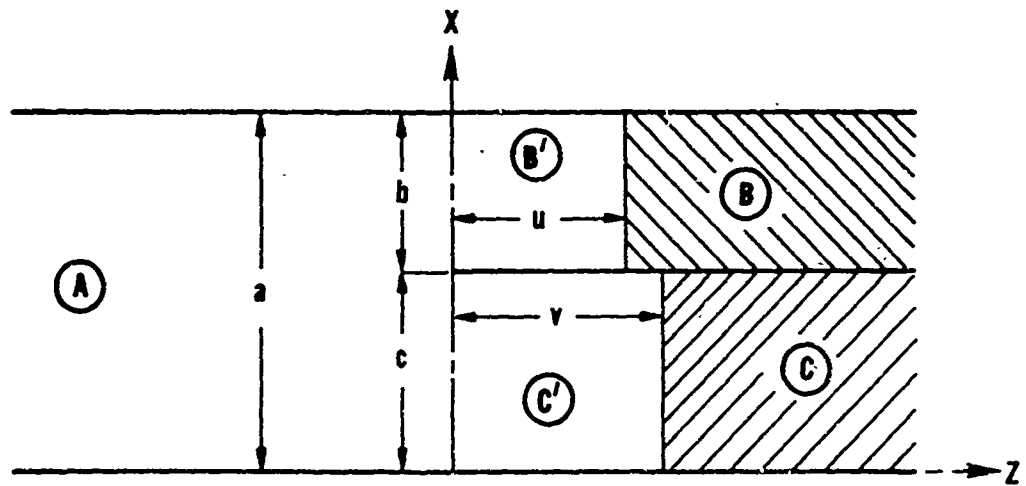


Figure 3.2 Auxiliary geometry for inhomogeneously-filled bifurcation

$$(A) \quad E_y = \sum_{n=1}^{\infty} A_n \sin(n\pi x/a) \exp(j\alpha_n z) + A \sin(p\pi x/a) \exp(-j\alpha_p z) \quad (3.2a)$$

$$(B') \quad E_y = \sum_{n=1}^{\infty} \sin(n\pi(x-c)/b) [B_n \exp(-j\beta_n z) + D_n \exp(j\beta_n z)] \quad (3.2b)$$

$$(B) \quad E_y = \sum_{n=1}^{\infty} F_n \sin(n\pi(x-c)/b) \exp(-j\bar{\beta}_n z) + B \sin(p\pi(x-c)/b) \exp(j\bar{\beta}_p z) \quad (3.2c)$$

$$(C') \quad E_y = \sum_{n=1}^{\infty} \sin(n\pi x/c) [C_n \exp(-j\gamma_n z) + E_n \exp(j\gamma_n z)] \quad (3.2d)$$

$$(C) \quad E_y = \sum_{n=1}^{\infty} G_n \sin(n\pi x/c) \exp(-j\bar{\gamma}_n z) \quad (3.2e)$$

where

$$\alpha_n = \sqrt{k_o^2 - (n\pi/a)^2}$$

$$\beta_n = \sqrt{k_o^2 - (n\pi/b)^2}$$

$$\gamma_n = \sqrt{k_o^2 - (n\pi/c)^2}$$

$$\bar{\beta}_n = \sqrt{\epsilon_b k_o^2 - (n\pi/b)^2}$$

$$\bar{\gamma}_n = \sqrt{\epsilon_c k_o^2 - (n\pi/c)^2}$$

$$k_o^2 = \omega^2 \mu_o \epsilon_o$$

Except for a constant factor, the transverse components of the magnetic field in the corresponding regions are found by partial differentiation with respect to z .

Matching tangential field components at $z = v$, $0 \leq x \leq c$, and equating Fourier coefficients yields

$$C_n \exp(-j\gamma_n v) + E_n \exp(j\gamma_n v) = G_n \exp(-j\bar{\gamma}_n v) \quad (3.3a)$$

$$\frac{1}{\omega\mu_0} [-\gamma_n C_n \exp(-j\gamma_n v) + \gamma_n E_n \exp(j\gamma_n v)] = -\frac{\bar{\gamma}_n}{\omega\mu_0} G_n \exp(-j\bar{\gamma}_n v) \quad (3.3b)$$

At $z = u$, $c \leq x \leq a$, a similar procedure yields

$$B_n \exp(-j\beta_n u) + D_n \exp(j\beta_n u) = F_n \exp(-j\bar{\beta}_n u) + \delta_n^D B \exp(j\bar{\beta}_p u) \quad (3.4a)$$

$$\begin{aligned} \frac{1}{\omega\mu_0} [-\beta_n B_n \exp(-j\beta_n u) + \beta_n D_n \exp(j\beta_n u)] \\ = \frac{1}{\omega\mu_0} [-\bar{\beta}_n F_n \exp(-j\bar{\beta}_n u) + \delta_n^D \bar{\beta}_p B \exp(j\bar{\beta}_p u)] \end{aligned} \quad (3.4b)$$

In the limit as $u \rightarrow 0$ and $v \rightarrow 0$, these equations can be simplified to give

$$E_n = \lambda_n C_n \quad (3.5a)$$

$$D_n = \xi_n B_n + \delta_n^D \frac{2\bar{\beta}_p}{(\beta_p + \bar{\beta}_p)} B \quad (3.5b)$$

where

$$\lambda_n = \left(\frac{\gamma_n - \bar{\gamma}_n}{\gamma_n + \bar{\gamma}_n} \right)$$

$$\xi_n = \left(\frac{\beta_n - \bar{\beta}_n}{\beta_n + \bar{\beta}_n} \right)$$

$\delta_n^D =$ Kronecker delta

For $u = v = 0$, the auxiliary and original geometry coincide, so that

the relations of (3.5a-b) may be used in formulation for regions (A), (B), and (C).

Matching tangential field components at the plane $z=0$ gives the following expressions:

$$A \sin(p\pi x/a) + \sum_{n=1}^{\infty} A_n \sin(n\pi x/a) =$$

$$\left\{ \begin{array}{l} \sum_{n=1}^{\infty} C_n (1+\lambda_n) \sin(n\pi x/c), \quad 0 \leq x \leq c \end{array} \right. \quad (3.6a)$$

$$\left\{ \begin{array}{l} \sum_{n=1}^{\infty} B_n (1+\xi_n) \sin(n\pi(x-c)/b) \end{array} \right.$$

$$+ 2 \frac{\bar{\beta}_p}{(\beta_p + \bar{\beta}_p)} B \sin(p\pi(x-c)/b), \quad c \leq x \leq a \quad (3.6b)$$

and

$$-c_p A \sin(p\pi x/a) + \sum_{n=1}^{\infty} \alpha_n A_n \sin(n\pi x/a) =$$

$$\left\{ \begin{array}{l} \sum_{n=1}^{\infty} \gamma_n C_n (-1+\lambda_n) \sin(n\pi x/c) \quad 0 \leq x \leq c \end{array} \right. \quad (3.7a)$$

$$\left\{ \begin{array}{l} \sum_{n=1}^{\infty} \beta_n B_n (-1+\xi_n) \sin(n\pi(x-c)/b) \end{array} \right.$$

$$+ 2 \frac{\beta_p \bar{\beta}_p}{(\beta_p + \bar{\beta}_p)} B \sin(p\pi(x-c)/b) \quad c \leq x \leq a \quad (3.7b)$$

Relations among the mode coefficients may be obtained by multiplying the equations above by $\sin(m\pi x/c)$ and $\sin(m\pi(x-c)/b)$ and integrating

in the respective regions $0 \leq x \leq c$ and $c \leq x \leq a$. Employing the integral identities

$$\int_0^c \sin(m\pi x/c) \sin(n\pi x/a) dx = (-1)^{m+1} \frac{m\pi}{c} \frac{\sin(n\pi c/a)}{\alpha_n^2 - \gamma_m^2}$$

and

$$\int_c^a \sin(m\pi(x-c)/b) \sin(n\pi x/a) dx = -\frac{m\pi}{b} \frac{\sin(n\pi c/a)}{\alpha_n^2 - \beta_m^2},$$

the relations for the mode coefficients become

$$\begin{aligned} A \frac{\sin(p\pi c/a)}{\alpha_p^2 - \gamma_m^2} + \sum_{n=1}^{\infty} A_n \frac{\sin(n\pi c/a)}{\alpha_n^2 - \gamma_m^2} \\ = (-1)^{m+1} \frac{c^2}{2m\pi} C_m (1 + \lambda_m) \end{aligned} \quad (3.8)$$

$$\begin{aligned} -\alpha_p A \frac{\sin(p\pi c/a)}{\alpha_p^2 - \gamma_m^2} + \sum_{n=1}^{\infty} \alpha_n A_n \frac{\sin(n\pi c/a)}{\alpha_n^2 - \gamma_m^2} \\ = (-1)^{m+1} \frac{c^2}{2m\pi} \gamma_m C_m (-1 + \lambda_m) \end{aligned} \quad (3.9)$$

$$\begin{aligned} A \frac{\sin(p\pi c/a)}{\alpha_p^2 - \beta_m^2} + \sum_{n=1}^{\infty} A_n \frac{\sin(n\pi c/a)}{\alpha_n^2 - \beta_m^2} \\ = -\frac{b^2}{2m\pi} B_m (1 + \xi_m) - \frac{b^2}{2p\pi} \frac{2\bar{\beta}_p}{(\beta_p + \bar{\beta}_p)} B \delta_m^p \end{aligned} \quad (3.10)$$

$$\begin{aligned}
& -\alpha_p A \frac{\sin(p\pi c/a)}{\alpha_p^2 - \beta_m^2} + \sum_{n=1}^{\infty} \alpha_n A_n \frac{\sin(n\pi c/a)}{\alpha_n^2 - \beta_m^2} \\
& = -\frac{b^2}{2m\pi} \beta_m B_m (-1 + \xi_m) - \frac{b^2}{2p\pi} \frac{2\bar{\beta}_p \beta_p}{(\beta_p + \bar{\beta}_p)} B_m^p
\end{aligned} \tag{3.11}$$

For simplification in notation, let

$$\bar{B} = 2 \frac{\bar{\beta}_p}{(\beta_p + \bar{\beta}_p)} B \tag{3.12a}$$

$$A'_n = A_n \sin(n\pi c/a) \tag{3.12b}$$

$$A' = A \sin(p\pi c/a) \tag{3.12c}$$

Equations (3.8-11) may be cast into more easily recognizable form by adding and subtracting multiples of the equations. The resultant equations are

$$\sum_{n=1}^{\infty} A'_n \left(\frac{1}{\alpha_n + \gamma_m} \right) - A' \left(\frac{1}{\alpha_p - \gamma_m} \right) + (-1)^{m+1} c^2 \gamma_m C_m / m\pi = 0 \tag{3.13}$$

$$\sum_{n=1}^{\infty} A'_n \left(\frac{1}{\alpha_n - \gamma_m} + \frac{\lambda_m}{\alpha_n + \gamma_m} \right) - A' \left(\frac{1}{\alpha_p + \gamma_m} + \frac{1}{\alpha_p - \gamma_m} \right) = 0 \tag{3.14}$$

$$\sum_{n=1}^{\infty} A'_n \left(\frac{1}{\alpha_n + \beta_m} \right) - A' \left(\frac{1}{\alpha_p - \beta_m} \right) - b^2 \beta_m B_m / m\pi = 0 \tag{3.15}$$

$$\sum_{n=1}^{\infty} A'_n \left(\frac{1}{\alpha_n - \beta_m} + \frac{\xi_m}{\alpha_n + \beta_m} \right) - A'_p \left(\frac{1}{\alpha_p + \beta_m} + \frac{\xi_m}{\alpha_p - \beta_m} \right) + \delta_m^p b^2 \beta_p \bar{B}/p\pi = 0 \quad (3.16)$$

These equations are valid for each $m = 1, 2, 3, \dots$. These simultaneous infinite sets of equations for the $\{A'_n\}$, $\{B_m\}$, and $\{C_m\}$ are in the general form discussed in Section II, hence approximate solution by the modified residue-calculus technique is possible. Because of the wide variety of possible variations on the basic geometry, the solution of the sets of equations will be discussed in general and then restricted cases of greater interest will be treated in detail.

Solution of the Sets of Equations

Because of the linearity of the system, it suffices to treat excitation from region (A) and region (B) separately. Excitation from region (A) is most applicable to specific cases of interest, so the discussion of the general solution will be in that context. Suppose, then, that $B=0$ and hence $\bar{B}=0$ in (3.16).

The inhomogeneous bifurcation is a generalization of the simple bifurcation in which $\epsilon_b = \epsilon_c = 1$. In the simple case, $\xi_m = \lambda_m = 0$, so that except for the factor A' , equations (3.14) and (3.16) reduce to (2.2) and (2.3), where the $\{A'_n\}$ are identified with the $\{A_n\}$. The solution is exactly as described in Section II except that the meromorphic function $g(w)$ is normalized to give $R_g(-\alpha_p) = A'$. Solution of the general case is based on modifications of the function $g(w)$ of (2.4).

Suppose that a meromorphic function $h(w)$ can be constructed which satisfies:

$$(h:1) \quad h(w) \text{ has simple poles at } w = -\alpha_p \text{ and at } w = \alpha_1, \alpha_2, \alpha_3, \dots$$

$$(h:2) \quad h(\beta_m) + \xi_m h(-\beta_m) = 0, \quad m = 1, 2, 3, \dots$$

$$(h:3) \quad h(\gamma_m) + \lambda_m h(-\gamma_m) = 0, \quad m = 1, 2, 3, \dots$$

$$(h:4) \quad h(w) \sim Kw^{-\nu}, \quad 4/3 \leq \nu \leq 5/3, \text{ as } |w| \rightarrow \infty. \quad (\text{The exact value of } \nu \text{ is determined by the edge condition and will be discussed subsequently.})$$

Consider the following integrals in the complex w -plane, where C is a closed contour enclosing all of the poles and zeros of $h(w)$.

$$\frac{1}{2\pi j} \oint_C \left(\frac{h(w)}{w+\gamma_m} \right) dw = \sum_{n=1}^{\infty} R_h(\alpha_n) \left(\frac{1}{\alpha_n+\gamma_m} \right) - R_h(-\alpha_p) \left(\frac{1}{\alpha_p-\gamma_m} \right) + h(-\gamma_m) = 0, \quad m = 1, 2, 3, \dots \quad (3.17)$$

$$\frac{1}{2\pi j} \oint_C \left(\frac{h(w)}{w-\gamma_m} + \lambda_m \frac{h(w)}{w+\gamma_m} \right) dw = \sum_{n=1}^{\infty} R_h(\alpha_n) \left(\frac{1}{\alpha_n-\gamma_m} + \frac{\lambda_m}{\alpha_n+\gamma_m} \right) - R_h(-\alpha_p) \left(\frac{1}{\alpha_p+\gamma_m} + \frac{\lambda_m}{\alpha_p-\gamma_m} \right) + h(\gamma_m) + \lambda_m h(-\gamma_m) = 0, \quad m = 1, 2, 3, \dots \quad (3.18)$$

$$\frac{1}{2\pi j} \oint_C \left(\frac{h(w)}{w+\beta_m} \right) dw = \sum_{n=1}^{\infty} R_h(\alpha_n) \left(\frac{1}{\alpha_n+\beta_m} \right) - R_h(-\alpha_p) \left(\frac{1}{\alpha_p-\beta_m} \right) + h(-\beta_m) = 0, \quad m = 1, 2, 3, \dots \quad (3.19)$$

$$\frac{1}{2\pi j} \oint_C \left(\frac{h(w)}{w-\beta_m} + \xi_m \frac{h(w)}{w+\beta_m} \right) dw = \sum_{n=1}^{\infty} R_h(\alpha_n) \left(\frac{1}{\alpha_n - \beta_m} + \frac{\xi_m}{\alpha_n + \beta_m} \right) - R_h(-\alpha_p) \left(\frac{1}{\alpha_p + \beta_m} + \frac{\xi_m}{\alpha_p - \beta_m} \right) + h(\beta_m) + \xi_m h(-\beta_m) = 0,$$

$$m = 1, 2, 3, \dots \quad (3.20)$$

When $h(w)$ is normalized to make $R_h(-\alpha_p) = A'$, (3.17-20) may be identified term by term with (3.13-16) to generate the solutions to the sets of equations. The results are:

$$A'_n = R_h(\alpha_n), \quad n = 1, 2, 3, \dots \quad (3.21)$$

$$C_m = (-1)^{m+1} \frac{m\pi}{c^2 \gamma_m} h(-\gamma_m), \quad m = 1, 2, 3, \dots \quad (3.22)$$

$$B_m = -\frac{m\pi}{b^2 \beta_m} h(-\beta_m), \quad m = 1, 2, 3, \dots \quad (3.23)$$

The required function $h(w)$ takes the form

$$h(w) = K \exp(Lw) \frac{\Pi(w, \beta') \Pi(w, \gamma')}{(w + \alpha_p) \Pi(w, \alpha)} \quad (3.24)$$

The zeros $\{\beta'_n\}$ and $\{\gamma'_n\}$ reduce to the zeros $\{\beta_n\}$ and $\{\gamma_n\}$ of $g(w)$ when $\lambda_m = \xi_m = 0$ (equivalently, $\varepsilon_b = \varepsilon_c = 1$). The constant L is given in (2.6) and the factor K is chosen to satisfy the normalization requirement. The nominal algebraic behavior of $h(w)$ is asymptotically $w^{-3/2}$, but corrections are made by the asymptotic shift of β'_n and γ'_n

from their nominal values of β_n and γ_n . Properties of the sets of zeros are determined concurrently by (h:2), (h:3), and the edge condition.

The solution for excitation from region (B) proceeds almost exactly as for excitation from (A). The function $h(w)$ differs in that the pole at $-\alpha_p$ and the zero at β'_p are eliminated, so that $h(w)$ maintains the same algebraic behavior as before. Subsequent arguments pertaining to the edge condition and asymptotic behavior carry over verbatim.

Edge Condition and Asymptotic Behavior of Zeros

So long as simple dielectrics ($\epsilon_d < \infty$, $\epsilon_c < \infty$) fill regions (B) and (C) and only TE excitation is considered, the inhomogeneously-filled waveguide bifurcation has the same edge behavior as the simple bifurcation. Thus, $h(w) \sim Kw^{-3/2}$ for both cases. However, two infinite sets of zeros must be determined simultaneously to satisfy (h:2) and (h:3). As in Section II, it is possible to extract information about the asymptotic zero positions by studying conditions (h:2) and (h:3) for large indices.

Suppose that for n very large, the propagation constants may be written

$$\alpha_n = -jn\pi/a$$

$$\beta_n = -jn\pi/b$$

$$\gamma_n = -jn\pi/c$$

$$\beta'_n = -jn\pi/b + S$$

$$\gamma'_n = -jn\pi/c + D$$

where S and D are the assumed asymptotic shifts of β'_n and γ'_n from the unshifted positions. Imposing (h:2) for m large in the form

$$h(\beta'_m)/h(-\beta'_m) = -\xi_m \text{ yields}$$

$$\begin{aligned} & \left(\frac{j m \pi / b + \alpha_p}{-j m \pi / b + \alpha_p} \right) \exp(-2j m \pi L / b) \frac{\prod(1 - \frac{-j m \pi / b}{-j n \pi / b + S})}{\prod(1 - \frac{+j m \pi / b}{-j n \pi / b + S})} \\ & \times \frac{\prod(1 - \frac{-j m \pi / b}{-j n \pi / c + D}) \prod(1 - \frac{+j m \pi / b}{-j n \pi / a})}{\prod(1 - \frac{+j m \pi / b}{-j n \pi / c + D}) \prod(1 - \frac{-j m \pi / b}{-j n \pi / a})} = -\xi_m \end{aligned} \quad (3.25)$$

The exponential convergence factors in the products have been omitted to simplify the appearance of the equation. When the products are replaced by their simplified forms from (2.20a) and (2.20b) and when the quotient containing α_p is replaced by its limiting value, equation (3.25) reduces to

$$\frac{\sin(m\pi - jSb) \sin(m\pi c / b - jDc)}{\sin(m\pi a / b)} = \frac{1}{2} \xi_m \quad (3.26)$$

Since $a = b + c$, this expression may be further reduced to

$$\frac{\sin(jSb) \sin(m\pi c / b - jDc)}{\sin(m\pi c / b)} = -\frac{1}{2} \xi_m \quad (3.27)$$

The corresponding result for (h:3) may be obtained from (3.27) upon interchanging b and c, S and D, and replacing ξ_m by λ_m .

$$\frac{\sin(jDc)\sin(m\pi b/c - jSb)}{\sin(m\pi b/c)} = -\frac{1}{2} \lambda_m \quad (3.28)$$

For simple dielectrics, both $\xi_m \rightarrow 0$ and $\lambda_m \rightarrow 0$ as $m \rightarrow \infty$. Thus, the R.H.S. of (3.27) and (3.28) tend to zero, and hence so must the L.H.S. if the equalities are to be maintained in the limit. This requirement is satisfied by $D = S = 0$, so that asymptotically the new zeros β'_n and γ'_n tend to the old zeros β_n and γ_n . The choice $S = D = 0$ is consistent with the edge condition, for no algebraic correction to the asymptotic behavior of $h(w)$ is permitted.

In the most general case, i.e., when one or both dielectrics assume limiting values as electric or magnetic conductors, such direct limiting arguments for (3.27) and (3.28) fail. They fail because the limits as $m \rightarrow \infty$ of the sine ratios fail to exist even though the R.H.S. of each equation does have a limiting value. Two cases of particular interest, namely the waveguide step and the diaphragm, may be solved as special limiting cases of the inhomogeneously-filled bifurcation. In those cases, limit difficulties with respect to asymptotic behavior of the zeros reflected in (3.27) and (3.28) can be circumvented by direct imposition of the edge condition. Although the two problems will be discussed in greater detail subsequently, the behavior of the set of zeros of $h(w)$ for their solution will be treated as special cases.

Case 1. When the dielectric in region (C) is allowed to become a perfect electric conductor and the dielectric in (B) remains simple, the geometry reduces to the waveguide step discontinuity of Figure 3.3.

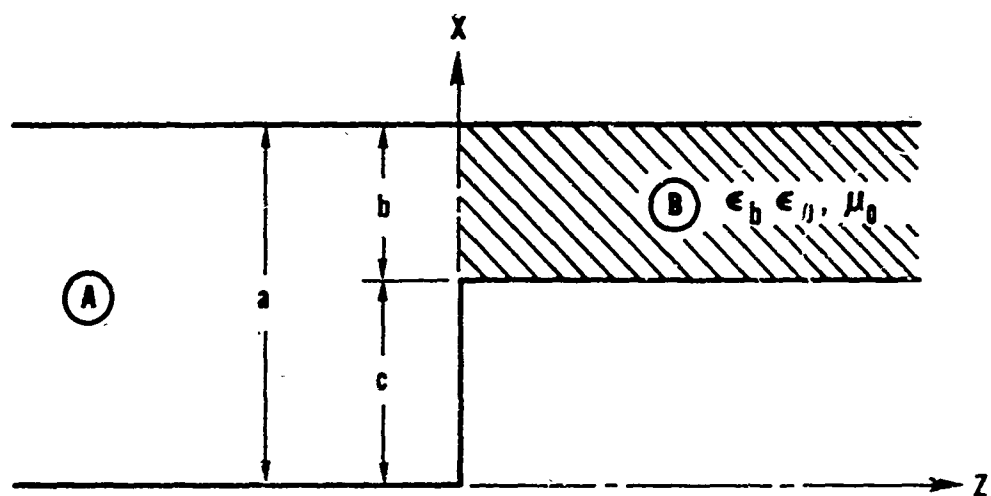


Figure 3.3 Waveguide step discontinuity

In this case, $\xi_n \rightarrow 0$ as $n \rightarrow \infty$, but $\lambda_n = -1$ for each n . The value of λ_n is readily interpreted as the n^{th} mode reflection coefficient at the interface between regions (C') and (C) in the auxiliary geometry of Figure 3.2. Naturally, when the dielectric becomes a perfect electric conductor, each mode reflection coefficient becomes -1 .

The limit of the R.H.S. of (3.27) is zero, but the R.H.S. of (3.28) is $+1/2$ for all n . The choice $S = 0$ reduces the L.H.S. of (3.27) to zero, so that (3.27) is satisfied in the limit. However, the choice $S = 0$ reduces (3.28) simply to

$$\sin(jDc) = \frac{1}{2} \quad (3.29)$$

which then implies that

$$D = -j\frac{\pi}{6c} \quad (3.30)$$

Thus the zeros $\{\gamma'_n\}$ are asymptotically shifted from $\{\gamma_n\}$ by the amount $D = -j\frac{\pi}{6c}$, but the asymptotic shift of the $\{\beta'_n\}$ is zero.

The edge condition for the waveguide step is that of a right-angle perfectly conducting wedge. The field behavior requires that $h(w) \sim Kw^{-5/3}$, which differs from the behavior for simple dielectrics by the factor of $w^{-1/6}$. It would appear at this point that a new form for $h(w)$ must be found to account for the new edge condition. However, the asymptotic shift of the zeros $\{\gamma'_n\}$ automatically incorporates the algebraic correction to $h(w)$.

The ratio $r(w)$ of $h(w)$ with shifted zeros to $h(w)$ with unshifted zeros is essentially

$$r(w) = \frac{\prod(1-w/(\gamma'_n+D))}{\prod(1-w/\gamma_n)} \quad (3.31)$$

However, substitution of asymptotic values for γ_n and reference to (2.20a) and (2.20b) yield a simpler expression for the ratio, namely

$$r(w) = \frac{\Gamma(1+jDc/\pi)\Gamma(1-j\pi c/\pi)}{\Gamma(1+jDc/\pi-j\pi c/\pi)\Gamma(1)} \quad (3.32)$$

From the asymptotic value of the ratio of gamma functions ($\Gamma(x+b)/\Gamma(x) \sim x^b$ as $x \rightarrow \infty$) given in Noble [1958], the ratio (3.32) becomes

$$r(w) \sim K(-j\frac{\pi c}{\pi})^{-j\frac{Dc}{\pi}} \quad (3.33)$$

Substitution of the asymptotic value of $D = -j\pi/6c$ yields

$$r(w) \sim K'w^{-1/6} \quad (3.34)$$

Thus the proper algebraic correction to $h(w)$ is automatically provided.

Case 2. When region (C) is filled with a perfect electric conductor and region (B) becomes a perfect magnetic conductor, the geometry reduces to a waveguide terminated by a combined magnetic and electric wall, as in Figure 3.4. Although this problem is essentially non-physical because magnetic conductors fail to exist, it is indeed useful as an auxiliary geometry for solving the problem of an inductive diaphragm in a waveguide. Its application to the diaphragm will be discussed subsequently.

The magnetic conductor in region (B) gives the value +1 for each ξ_m . As in Case 1, $\lambda_m = -1$ for each m . Unlike Case 1, however, the limiting procedure applied to (3.27) and (3.28) fails completely, indicating that the zeros fail to have a specific asymptotic shift,

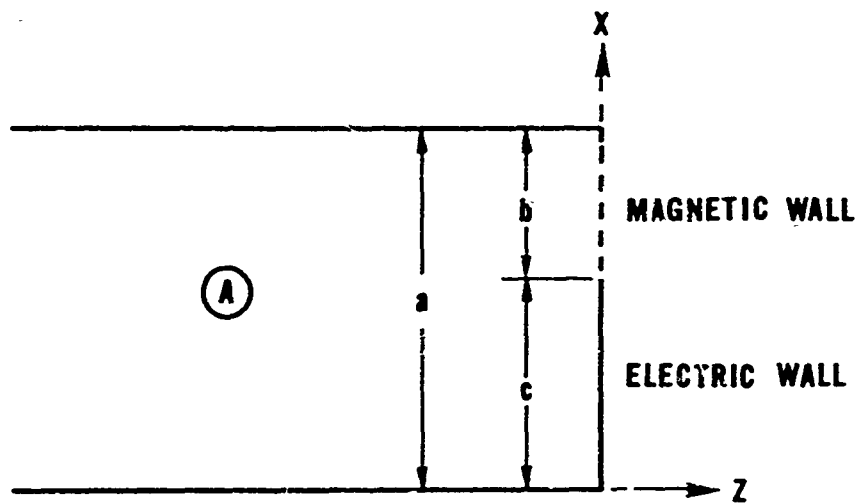


Figure 3.4 Magnetic-wall, electric-wall termination

except possibly in an average sense. Fortunately, though, the edge condition for Case 2 is known exactly, so that edge condition information can be used to advantage.

Because the geometry of Case 2 may be directly related to the inductive diaphragm, the edge condition is that of the diaphragm, which like the simple bifurcation, requires $h(w) \sim Kw^{-3/2}$. Since no algebraic correction to $h(w)$ is required, the edge condition alone yields

$$S = 0 \quad (3.35a)$$

$$D = 0 \quad (3.35b)$$

for the asymptotic shifts of the zeros. Since the conditions (h:2) and (h:3) for the magnetic-electric wall case are somewhat stronger, it may very well require longer for the actual zeros to approach the asymptotic values. However, because the actual shifts of the first few zeros of $h(w)$ are found explicitly, the numerical results for scattering matrix elements for low-order modes are quite insensitive to errors in the location of large-order zeros of $h(w)$, hence in S and D .

The essential test of the proper choice of asymptotic shifts is the satisfaction of (h:2) and (h:3). Of course, when the conditions assume proper limiting forms, the problem is greatly simplified. However, arguments such as those for Case 2 may be invoked when direct limiting procedures fail. In some cases, moreover, explicit computation of exact zero locations may lead to a numerical determination of the asymptotic shift of large-index zeros. In all, any reasonable

means that yields satisfaction of (h:2) and (h:3) and the edge condition may be useful.

Construction of $h(w)$

Since the functional form of $h(w)$ is known exactly, construction of $h(w)$ consists in determining the unknown zeros. As in the problem discussed in Section II, it is not possible to determine all of the zeros exactly. Again it suffices to substitute asymptotic values for all but the first few values of β'_n and γ'_n and to find the first values explicitly. Suppose that M_B values of β'_n and M_C values of γ'_n are to be found explicitly, and that $M = M_B + M_C$. Actually, a polynomial of order M is determined since exact location of the zeros is irrelevant. The function may be written

$$h(w) = K P(w) \frac{\exp(Lw) \Pi^{(M_B)}(w, \beta') \Pi^{(M_C)}(w, \gamma')}{(w + \alpha_p) \Pi(w, \alpha)} \quad (3.36)$$

where $\Pi^{(M_B)}(w, \beta')$ denotes omission of the first M_B factors and replacement of β'_n by $\beta'_n + S$ for $n > M_B$, and similarly for $\Pi^{(M_C)}(w, \gamma')$.

$P(w)$ is a polynomial of order M . For simplicity, write

$$h(w) = K P(w) h'(w) \quad (3.37)$$

where $h'(w)$ incorporates all of the known parts of $h(w)$.

Although the method of determining directly the polynomial coefficients which is described in Section II is perfectly applicable to this case, an alternative method of specifying $P(w)$ is superior for numerical work, albeit more complicated. The method consists of writing $P(w)$ as a known polynomial of order M plus a correction

polynomial of order $M-1$. For convenience in notation, let

$$W_i = \beta_i, \quad i = 1, 2, \dots, M_B$$

$$W_{i+M_B} = \gamma_i, \quad i = M_B+1, M_B+2, \dots, M_B + M_C = M$$

$$t_i = \xi_i, \quad i = 1, 2, \dots, M_B$$

$$t_{i+M_B} = \lambda_i, \quad i = M_B + 1, M_B + 2, \dots, M$$

Thus, conditions (h:2) and (h:3) for the explicitly shifted zeros read:

$$h(W_i) + \tau_i h(-W_i) = 0, \quad i = 1, 2, \dots, M \quad (3.38)$$

Now write $P(w)$ in the following form:

$$P(w) = \prod_{i=1}^M (1-w/W_i) + \sum_{i=1}^M [F_i \prod_{\substack{j=1 \\ j \neq i}}^M \frac{w-W_j}{W_i-W_j}] \quad (3.39)$$

The first term of $P(w)$ is readily recognizable as the product of unshifted zeros. The second term, in which the coefficients F_i ,

$i = 1, 2, \dots, M$, are to be found, forms the correction polynomial.

The normalization of the second term is such that $P(W_i) = F_i$, $i = 1, 2, \dots, M$.

Substituting the new form of $P(w)$ into (3.38) yields

$$K h'(W_m) F_m + \tau_m K h'(W_m) \left\{ \prod_{i=1}^M (1+W_m/W_i) \right.$$

$$\sum_{i=1}^M [F_i \prod_{\substack{j=1 \\ j \neq i}}^M \left(\frac{-W_m - W_j}{W_i - W_j} \right)] = 0, \quad m = 1, 2, 3, \dots, M \quad (3.40)$$

Since the only unknowns are the $\{F_i\}$, which appear linearly, (3.40) is actually a set of M simultaneous linear equations for the $\{F_i\}$. Solution of such sets by numerical methods is well-known. In actual practice, Gauss-Jordan elimination in double-precision complex arithmetic was used on an IBM-7094 digital computer.

The advantage of this scheme for finding the polynomial is that the unknowns are of first-order, while the unknown polynomial coefficients in the direct method are of zero-order. The alternative method reduces to $F_i = 0$, $i = 1, 2, 3, \dots, M$, when the geometry reduces to a simple bifurcation; for the same case, the direct method yields rather large values for the unknowns. The best test of the polynomial determination is the satisfaction of (h:2) and (h:3), or equivalently, (3.38). The correction polynomial method is consistently superior to the direct polynomial method in satisfying (3.38) numerically.

Application to Specific Examples

Simple dielectric fillings. Apart from the homogeneous bifurcation, the simplest geometry is that of Figure 3.1, in which regions (B) and (C) are filled with simple dielectrics. For a fixed waveguide width a , the reflection coefficient varies with the position of the septum (i.e., with the ratio c/a). Over intervals in which both guide (B) and guide (C) are cut off, the magnitude of the

reflection coefficient is unity. Because the cut-off dimension also varies with the nature of the dielectric filling, the interval of total reflection varies with the dielectric constant. Figure 3.5 illustrates the cut off phenomenon for a singly-filled bifurcation. Region (C) is filled with a dielectric ϵ_c , but region (B) is unfilled. For the guide dimension $a = 0.75\lambda$, the reflection coefficient for the TE_{10} mode from (A) is given for $\epsilon_c = 1.0, 2.0,$ and 3.0 . Note the coincidence of the reflection coefficients up to the point $c/a = 0.33$ at which point the unfilled guide (B) cuts off. Also of interest are the limiting values as $c/a = 1$, in which cases the junction becomes that between an unfilled guide and a filled guide of identical dimension. The cut off points for the guide (C) are readily observable as break-points in the curves of Figure 3.5. Both magnitude and phase of the reflection coefficient for discrete values of c/a for the same geometry are given in Table 3.1.

Reflection coefficients for the doubly-filled bifurcation are depicted in Figure 3.6. In each case, guide (B) is filled with a dielectric $\epsilon_b = 3.0$, while results are given for $\epsilon_c = 1.0, 2.0,$ and 3.0 . Again break-points in the curves may be identified with cut off dimensions in the waveguide. As before, $a = 0.75\lambda$.

Step discontinuity. Of greater practical importance than the simple dielectric-filled bifurcation is the waveguide step discontinuity of Figure 3.3. Extensive results for step discontinuities of various kinds are given in Marcuvitz [1951], where primarily variational techniques are employed to find the dominant mode reflection coefficient and equivalent circuit reactance. However, no results

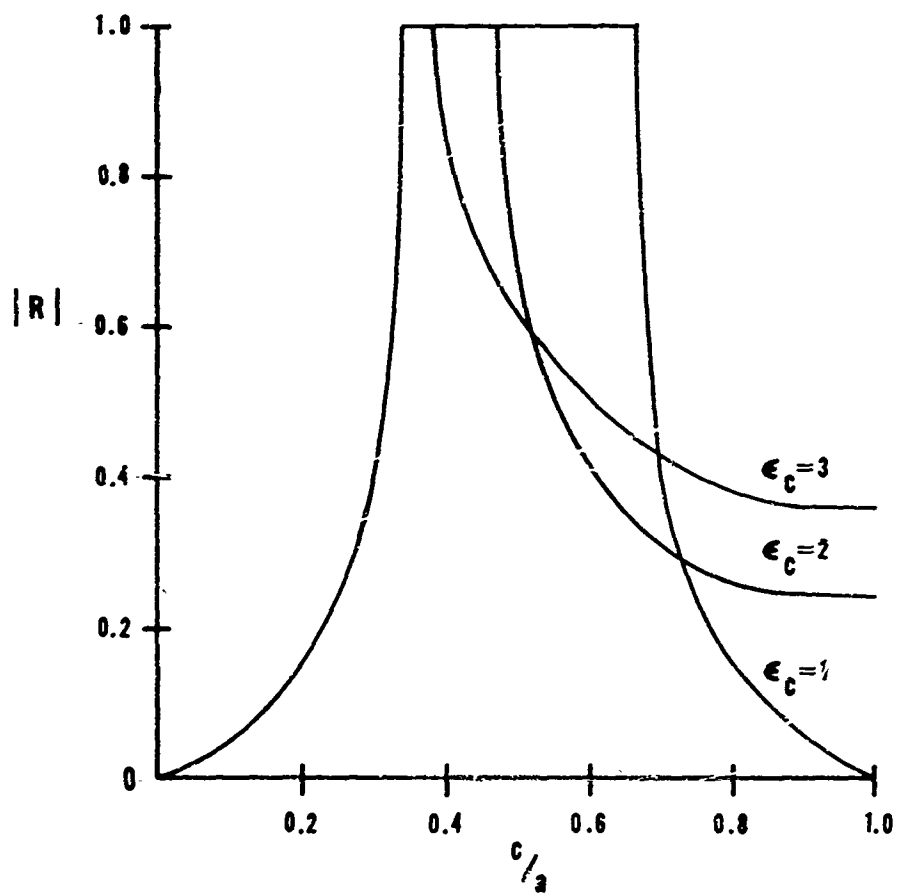


Figure 3.5 Reflection coefficient for inhomogeneously-filled bifurcation ($\epsilon_b = 1.0$, $a = 0.75\lambda$)

TABLE 3.1

Reflection Coefficient for Inhomogeneously-Filled Bifurcated Waveguide

c/a	Reflection Coefficient (Magnitude, Angle)		
	$\epsilon_c=1.0, \epsilon_b=1.0$	$\epsilon_c=2.0, \epsilon_b=1.0$	$\epsilon_c=3.0, \epsilon_b=1.0$
0.0	0.	0.	0.
0.1	(0.051, 36.3°)	(0.051, 36.1°)	(0.051, 36.1°)
0.2	(0.148, 50.6°)	(0.148, 50.5°)	(0.147, 50.3°)
0.3	(0.420, 53.6°)	(0.420, 53.1°)	(0.416, 52.5°)
0.4	(1.000, 112.3°)	(1.000, 109.1°)	(0.847, 100.6°)
0.5	(1.000, 127.2°)	(0.656, 110.8°)	(0.620, 134.3°)
0.6	(1.000, 112.3°)	(0.417, 135.5°)	(0.510, 152.0°)
0.7	(0.420, 53.6°)	(0.318, 151.8°)	(0.433, 162.5°)
0.8	(0.148, 50.6°)	(0.264, 164.5°)	(0.371, 170.5°)
0.9	(0.051, 36.3°)	(0.244, 174.8°)	(0.358, 177.7°)
1.0	0.	(0.252, 180.0°)	(0.365, 180.0°)

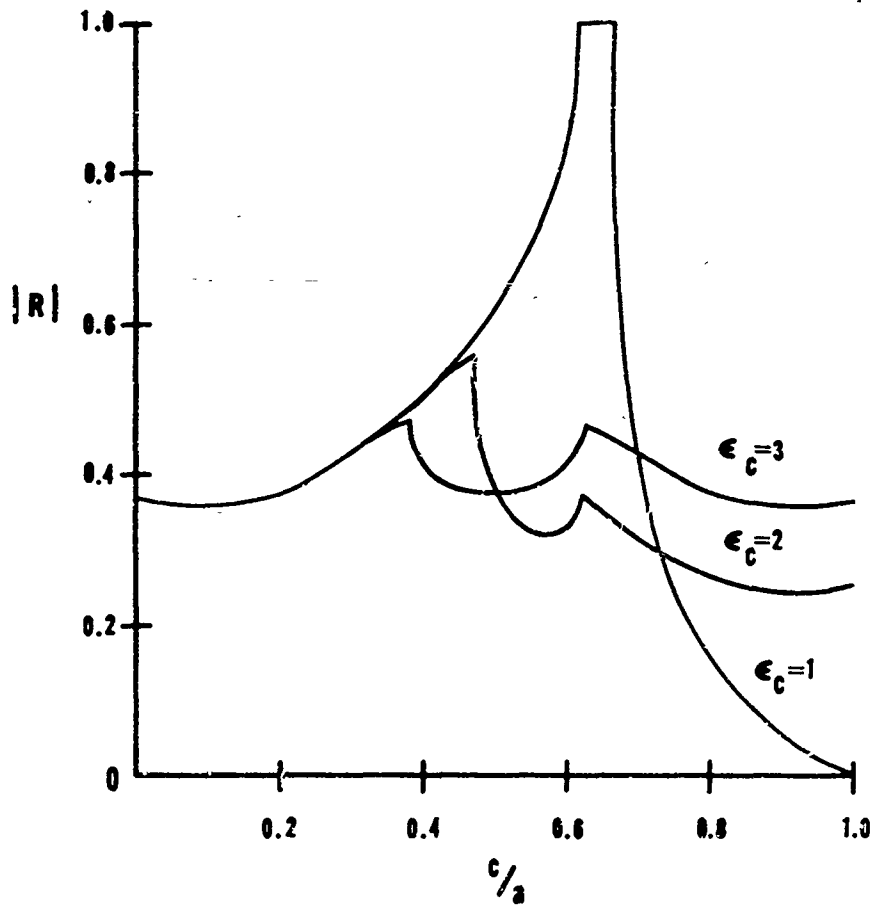


Figure 3.6 Reflection coefficient for inhomogeneously-filled bifurcation ($\epsilon_b = 3.0$, $a = 0.75\lambda$)

seem to be given for the junction of guides of different dimension and different dielectric filling, which is the most general case of Figure 3.3.

Because the step discontinuity is merely an extension of the inhomogeneously-filled bifurcation, scattering matrix representations of the discontinuity can be readily found by the MRCT. Although it often suffices to determine only the dominant mode reflection coefficients, knowledge of the scattering matrices, even though truncated at a small size ($N=5$, for example), makes possible very simple solutions of such problems as the thick-wall phased array (Section IV). In addition, knowledge of the high-order mode coefficients for the scattered field permit very accurate determination of the electric or magnetic field at the discontinuity. An example of the truncated scattering matrix S^{AA} for a step discontinuity is given in Table 3.2. The guide width $a = 0.75\lambda$ and $c/a = 0.3$; region (B) is unfilled.

Even though only a very small number of zeros of the function $h(w)$ are determined explicitly in the solution of the step problem, availability of approximate values for the high-order mode coefficients permits computation of the electric field at the plane $z = 0$. Assume that a TE_{10} mode of unit amplitude is incident from region (A). The coefficients of the first twenty reflected modes are found by the MRCT and the total field is calculated from the truncated Fourier series at $z = 0$. The amplitudes of total electric field for step widths of $0.2a$, $0.3a$, $0.4a$, and $0.5a$ are shown in Figure 3.7. It is important to note that the fields are computed in region (A), so that

TABLE 3.2
Truncated Scattering Matrix S^{AA} for Waveguide Step Discontinuity

($a = 0.75\lambda$, $c/a = 0.3$)

(0.1900 + j0.3538)	(-0.1882 + j0.7856)	(-0.1542 + j0.2814)	(-0.0016 - j0.1123)	(0.1079 - j0.3000)
(-0.6616 - j0.1585)	(-0.6131 - j0.4392)	(-0.4496 - j0.1526)	(-0.1569 + j0.0643)	(0.1020 + j0.1658)
(-0.1120 - j0.0657)	(-0.2276 - j0.0773)	(-0.2924 - j0.0314)	(-0.2736 + j0.0098)	(-0.1762 + j0.0310)
(0.0333 - j0.0005)	(-0.0552 + j0.0226)	(-0.1901 + j0.0060)	(-0.3049 - j0.0037)	(-0.3210 - j0.0081)
(0.0684 + j0.0246)	(0.0276 + j0.0449)	(-0.0942 + j0.0166)	(-0.2470 - j0.0062)	(-0.3388 - j0.0173)

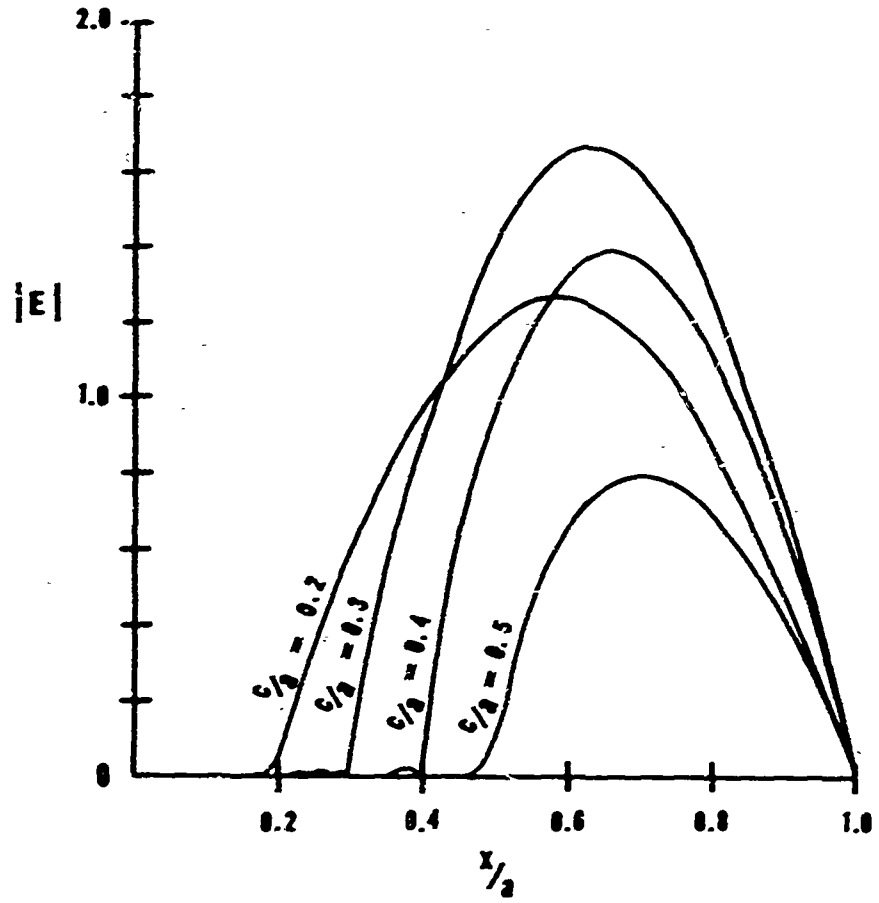


Figure 3.7 Amplitude of aperture electric field ($a = 0.75\lambda$)

the extremely small value (almost zero) of the field from $x = 0$ to $x = c$ for each case illustrates the satisfaction of the requirement $E_{\tan} = 0$ on $x = 0$ to $x = c$ for even the truncated series. Comparison of the fields in the aperture $c \leq x \leq a$ as computed in region (A) with the corresponding values computed in region (B) have shown agreement to several significant figures. Although the mode coefficients found by the MRCT are only approximate, the field found from them is probably very near to a least-mean-square approximation to the actual value because of the Fourier-Bessel inequality.

The reflection coefficient as a function of relative step width c/a is shown in Figure 3.8. Region (B) is filled with dielectric $\epsilon_b = 1.0, 2.0,$ and 3.0 . The guide width $a = 0.75\lambda$. The limiting case $c/a = 0$ yields the reflection coefficient for the air-dielectric interface in a waveguide; the case $c/a = 1$ yields the reflection coefficient -1 for a shorted waveguide. As previously, the break points in the magnitude and phase curves occur as guide (B) cuts off.

Magnetic and electric wall. The magnetic wall-electric wall termination of a waveguide illustrated in Figure 3.4 may be solved by the MRCT as discussed under Case 2. The geometry of Figure 3.4 is useful as an auxiliary geometry in the solution of the waveguide diaphragm of Figure 3.9. An additional auxiliary geometry is the shorted waveguide, the solution of which is trivial.

Consider equal excitation of the diaphragm of Figure 3.9 from regions (A) and (A') in a symmetric sense, i.e., with electric vectors in both regions pointing in the same direction. Then at the plane $z = 0$, the electric vectors add in the aperture and vanish on the

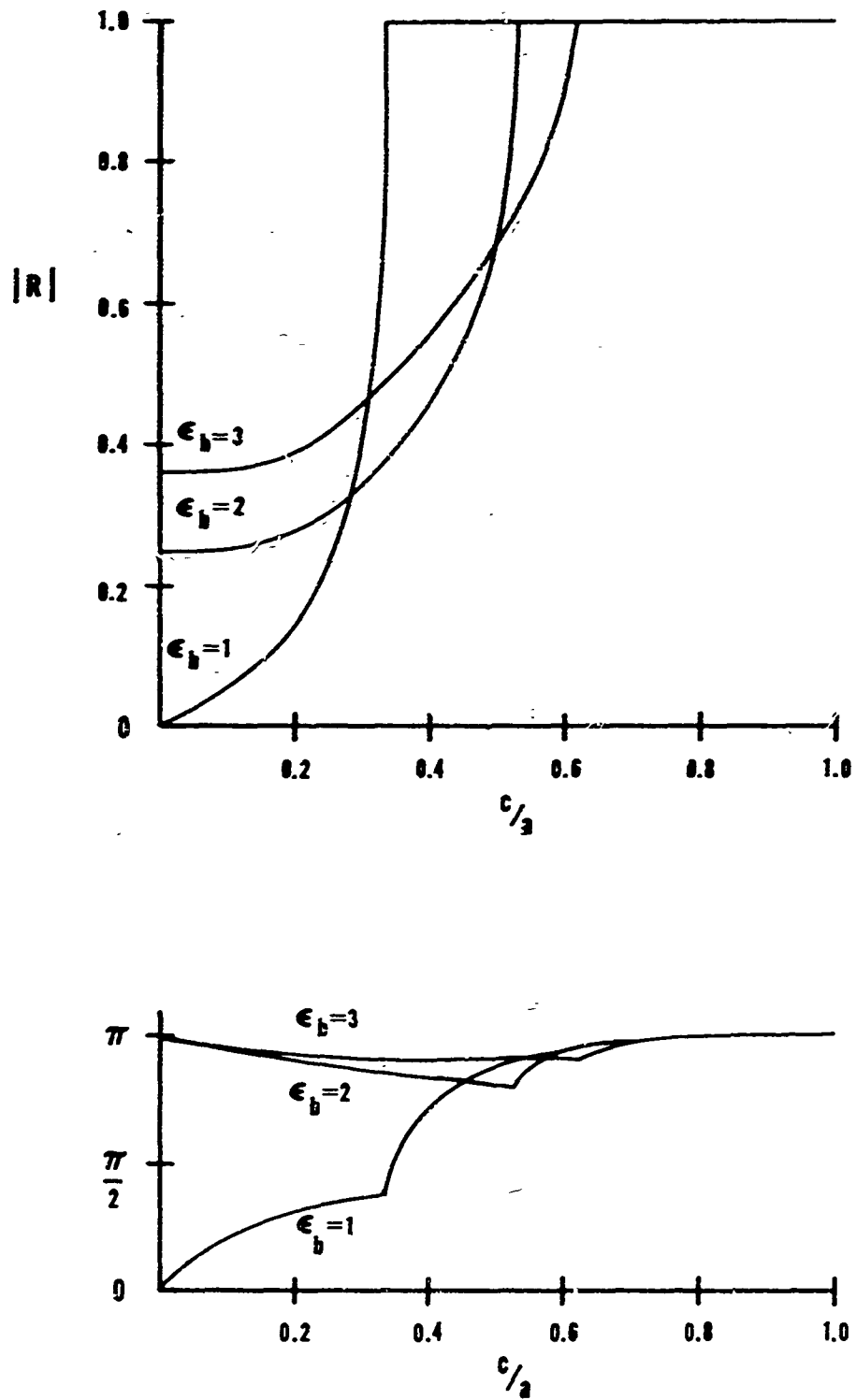


Figure 3.8 Reflection coefficient for waveguide step discontinuity ($a = 0.75\lambda$)

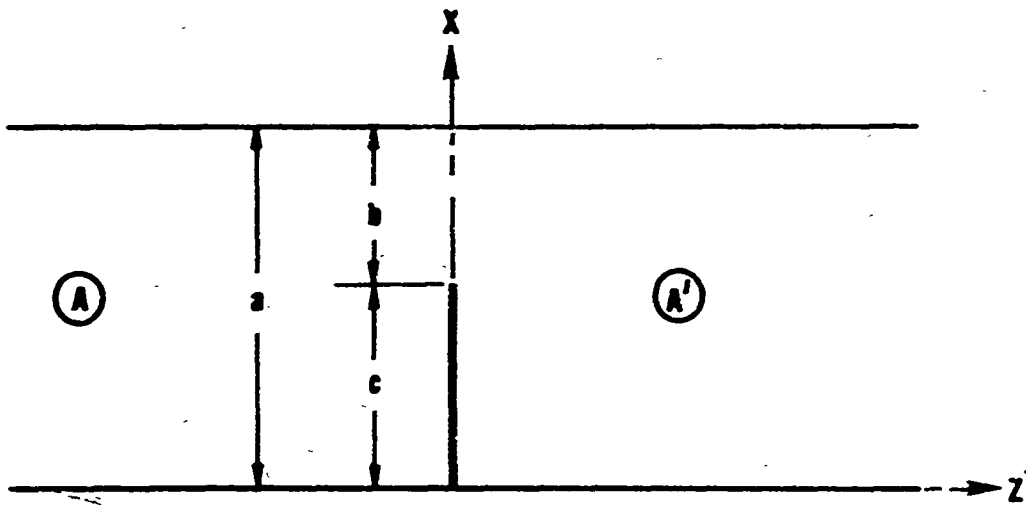


Figure 3.9 Waveguide inductive diaphragm

diaphragm, but the transverse magnetic vectors cancel exactly in the aperture. Thus placement of a magnetic wall in the aperture has no effect on the fields, and so far as region (A) is concerned, the geometry is that of Figure 3.4. Alternative equal but antisymmetric excitation of the diaphragm from (A) and (A') causes the total electric vector to vanish on the plane $z = 0$, so that an electric wall may be placed there without effect. Then, the geometry for region (A) reduces to a shorted waveguide.

Suppose, now, that both symmetric and antisymmetric excitation are applied to the diaphragm simultaneously, so that addition occurs in (A) but exact cancellation occurs in (A'). Let S_1^{AA} be the scattering matrix determined approximately for the magnetic-electric wall, and let $S_2^{AA} = -I$ be the scattering matrix for the shorted waveguide. Then the resultant scattering matrix S^{AA} for the diaphragm is given by

$$S^{AA} = \frac{1}{2}(S_1^{AA} + S_2^{AA}) = \frac{1}{2}(S_1^{AA} - I) \quad (3.41)$$

If R_1 is the complex reflection coefficient for the dominant mode for the magnetic-electric wall, then the reflection coefficient, R for the diaphragm of the same dimension is

$$R = \frac{1}{2}(R_1 - 1) \quad (3.42)$$

Because no power is transmitted beyond the magnetic-electric wall, the magnitude of R_1 is always exactly unity. The phase changes from 0 to π as the ratio c/a goes from 0 to 1. The magnitude and phase of R as

a function of c/a for the diaphragm is given in Figure 3.10. The guide width is $a = 0.75\lambda$.

An additional application of the scattering matrix description of the magnetic-electric wall geometry is diffraction by an infinite array of thin conducting strips. This problem is discussed in Section V.

Alternative Solution Methods

By the very nature of the geometry of the problems related to the simple waveguide bifurcation, it is apparent that alternative methods of solution exist. The generalized scattering matrix procedure is directly applicable to many of the problems, since the geometries can often be reduced to combinations of exactly solvable junctions. Variational and integral equation methods such as those described by Marcuvitz [1951] have been applied with success to many such problems. In any specific instance, the choice of method of solution can be made in many ways.

As applied to geometries related to the waveguide bifurcation, the modified residue-calculus technique possesses some great advantages. First, it is extremely general. All of the problems discussed in this section were solved by use of the same computer program, whether the problem was the simple bifurcation to be solved exactly or the magnetic-electric wall. Second, it generates scattering matrix representations of discontinuities, such as those obtained by the multiple-reflection, Neumann-series method. On the other hand, it can generate the first M scattered mode coefficients for the first incident mode without resorting to an $M \times M$ matrix inversion. Inversion

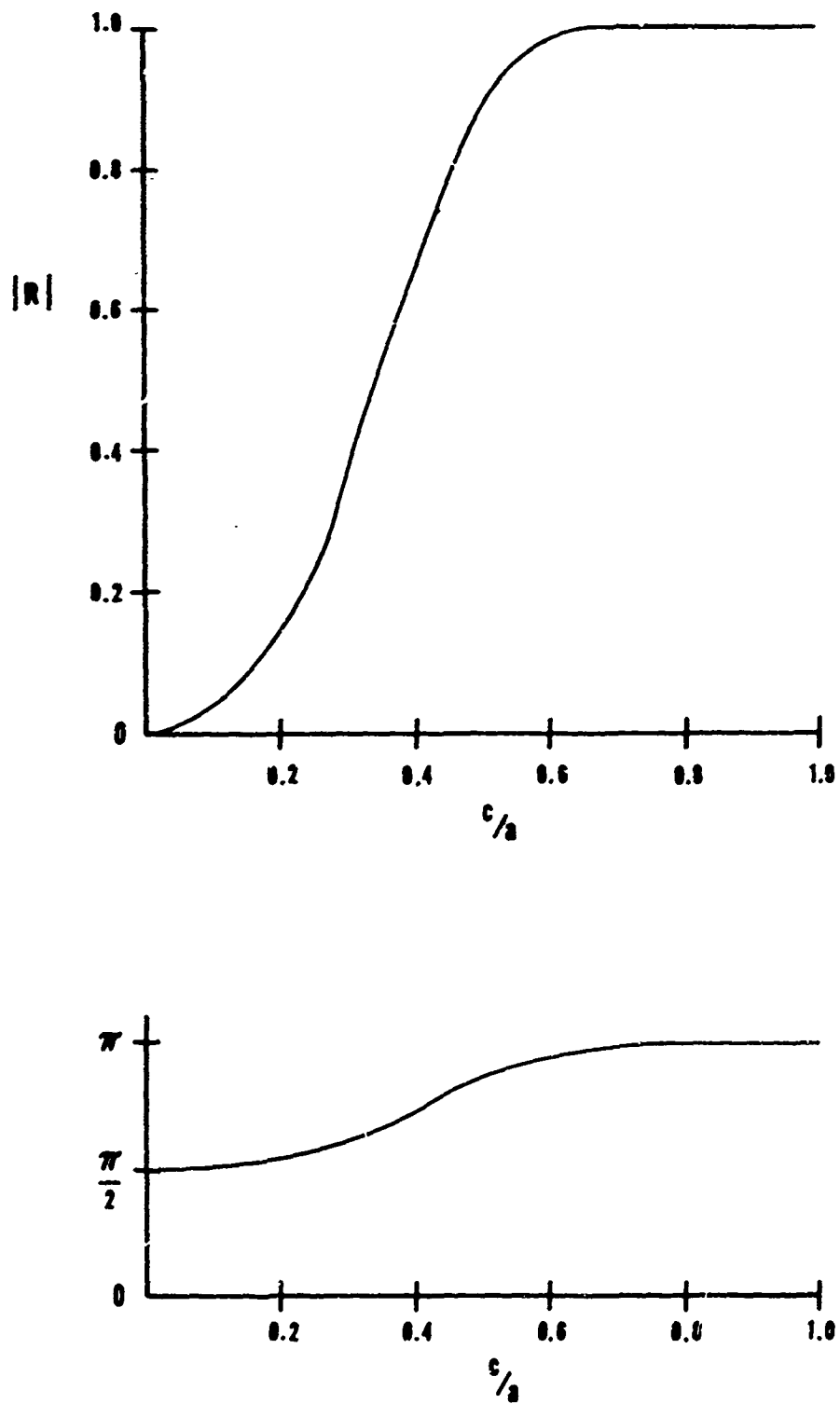


Figure 3.10 Reflection coefficient for waveguide diaphragm discontinuity

of large-order matrices is a major drawback to some methods in the solution of integral equations. Not least important is the automatic satisfaction of the edge condition. In both direct matrix inversion methods as well as the generalized scattering matrix method, it is difficult to prove directly that the edge condition is satisfied. In the MRCT, satisfaction is *a priori* guaranteed.

IV. THICK-WALL PHASED ARRAY

At the present time, there is great interest in antennas which are physically stationary but which electronically scan a relatively narrow beam throughout a region of space. Two particular applications are radio telescopes, in which the antenna is often so large that mechanical steering is prohibitively difficult, and tracking radars, in which a physical antenna has too great inertia to be rapidly and repeatedly scanned over a large area while tracking several fast-moving targets. In electronically scanned antennas, phase changes between elements steer the antenna beam without need for mechanical positioning.

One type of electronically scanned antenna is a phased array of open-end rectangular waveguides, a segment of which is shown in Figure 4.1. Although the number of elements (waveguides) in such an array is necessarily finite, it is not uncommon in practice for the number of elements to be extremely large. For purposes of analysis, it is convenient to assume that the array is infinite in extent and periodic. The infinite array approximation is good for the majority of elements away from the edges of the finite array. It is further assumed that the waveguides are excited by the dominant TE mode with uniform amplitude and periodic phasing to scan the beam. To be determined for the array are the aperture fields, from which the radiation pattern may be computed, and the reflection coefficient for the dominant mode in each waveguide as a function of scan angle.

The infinite rectangular array was discussed by Wu and Galindo [1966] for H-plane and quasi-E-plane scan for infinitely thin

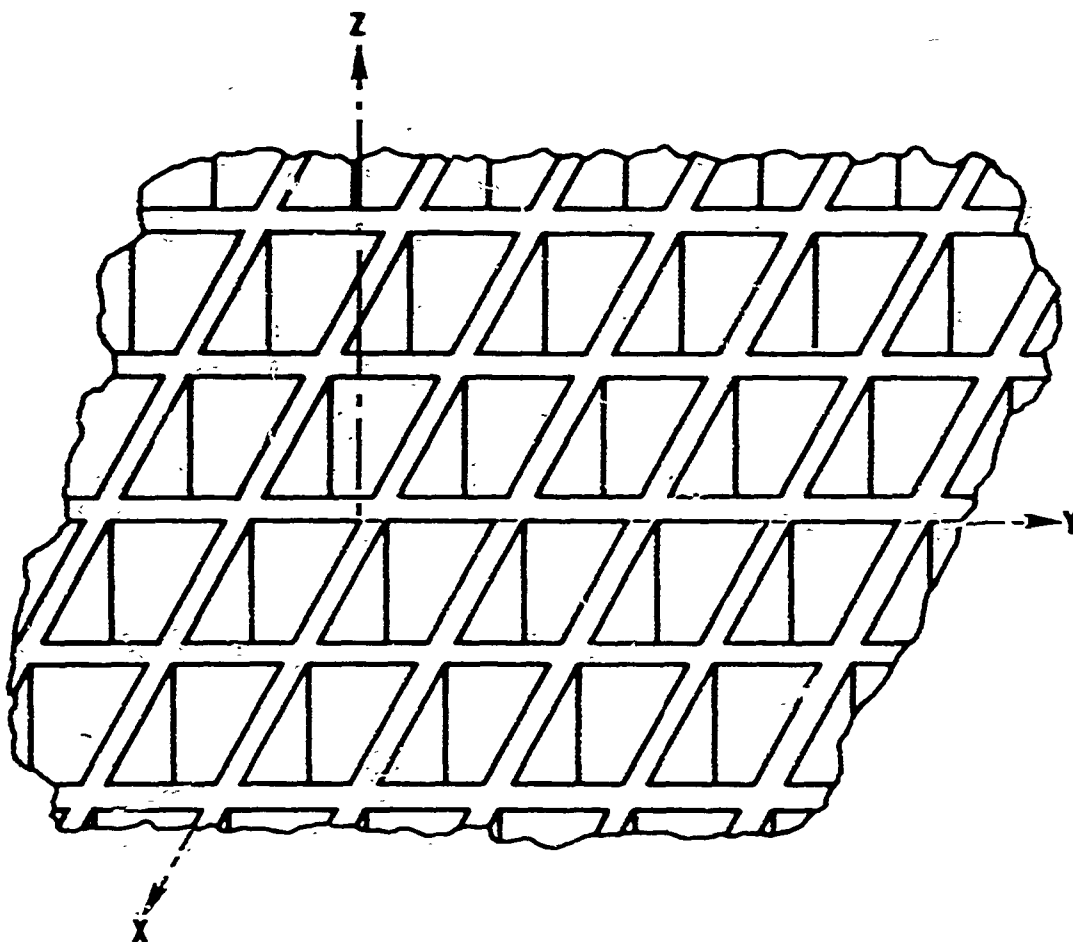


Figure 4.1 Phased array of open-end rectangular waveguides

waveguide walls and by Galindo and Wu [1965] for walls of finite thickness. The case of thin walls and H-plane scan is equivalent to diffraction by an infinite set of thin parallel plates, which may be solved exactly by the Wiener-Hopf technique (Carlson and Heins [1947]) or by the conventional residue-calculus technique (Berz [1951], Whitehead [1951]). However, the corresponding problem with walls of non-zero thickness cannot be solved exactly. Radiation at broadside from an array of thick plates was studied by Lee [1957], who presented a solution based on the Wiener-Hopf technique. By a numerical solution to an integral equation for the aperture field, Galindo and Wu [1966] were able to find reflection coefficients and aperture fields for several cases of wall thickness and waveguide dimension for angles of scan from 0° to 90° .

Not unexpectedly, the results of Galindo and Wu indicate that the reflection coefficient solutions for the thin wall array are not very good approximations to the reflection coefficients for arrays with walls of non-zero thickness. Because a major consideration in array design is to minimize reflection at the aperture, it is essential to know the variation of reflection coefficient with wall thickness and, in some circumstances, with the dielectric properties of the material filling the waveguide. (A technique sometimes used to match an array is to fill the waveguides with dielectric material.) But, it is extremely useful to determine the required information in the simplest possible way, so that as little time as possible is consumed in determining the required array characteristics.

Because of the nature of the array geometry, fields in each region may be written in modal expansions. As a result, the reflection and transmission characteristics of the array may be completely described by a set of scattering matrices. Since the model for the array may be reduced to two auxiliary junction problems, the generalized scattering matrix procedure may be readily applied to the array geometry. The MRCI solution of one of the related junction problems makes possible an extremely simple solution to the array problem. In particular, it permits determination of an approximate expression for the dominant mode reflection coefficient in a form suitable for simple hand calculation from data available in tabular or graphical form.

Thin-wall Array

The solution for the array with thin walls and H-plane scan forms the basis for the solution of the corresponding thick-wall array. As previously mentioned, this problem was discussed in detail by Wu and Galindo [1966], who obtained an exact solution for dominant mode excitation by means of the conventional residue-calculus technique. Because solution in terms of a generalized scattering matrix is essential to further results, the solution for the thin-wall array with general TE excitation will be summarized here.

The thin-wall array for H-plane scan is equivalent to a set of thin, perfectly conducting plates uniformly spaced (Figure 4.2). Each parallel plate waveguide thus formed is excited in the region $z < 0$ by a $TE_{p,0}$ mode of unit amplitude. The electric field in the m^{th} waveguide (region (A)) may be written

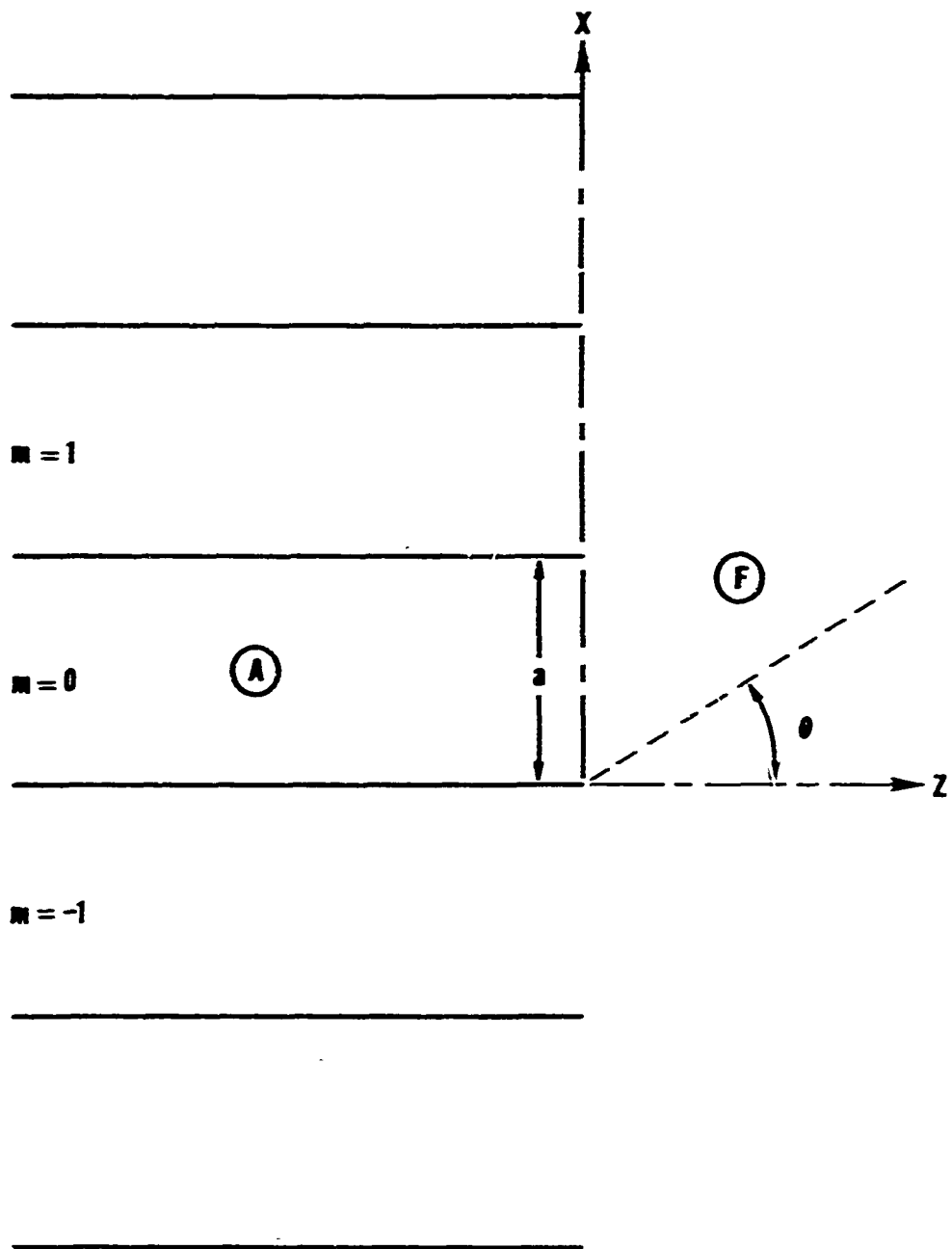


Figure 4.2 Infinite array of thin parallel plates

$$\begin{aligned}
 E_y &= \sin\left(\frac{p\pi}{a}(x-za)\right) \exp(-j\pi u - j\alpha_p z) \\
 &+ \sum_{n=1}^{\infty} A_n \sin\left(\frac{n\pi}{a}(x-za)\right) \exp(-j\pi u + j\alpha_n z)
 \end{aligned} \tag{4.1}$$

and in the open region (F)

$$E_y = \sum_{n=-\infty}^{\infty} G_n \exp(-j\xi_n x - j\tau_n z) \tag{4.2}$$

where

$$u = k_0 a \sin \theta$$

$$\xi_n = (2n\pi + u)/a$$

$$\tau_n = \sqrt{k_0^2 - \xi_n^2}$$

$$\alpha_n = \sqrt{k_0^2 - (n\pi/a)^2}$$

Space modes for which τ_n has a non-zero real part propagate away from the array and carry real power. The number of propagating space modes is a function of both guide width a and scan angle θ . Expressions proportional to the transverse magnetic field H_x are found by differentiating (4.1) and (4.2) with respect to z .

Upon matching the transverse field components at $z = 0$ and Fourier analyzing the resultant expressions as described in Section III, the following infinite sets of equations are obtained:

$$\begin{aligned}
 \sum_{n=1}^{\infty} n A_n [(-1)^n \exp(ju) - 1] \left(\frac{1}{\alpha_n - \tau_n} \right) \\
 - p [(-1)^p \exp(ju) - 1] \left(\frac{1}{\alpha_p + \tau_p} \right) = 0
 \end{aligned} \tag{4.3}$$

$$\sum_{n=1}^{\infty} n A_n [(-1)^n \exp(ju)-1] \left(\frac{1}{\alpha_n + \tau_q} \right) - p [(-1)^p \exp(ju)-1] + 2 \frac{a^2}{\pi} \tau_q G_q = 0 \quad (4.4)$$

The solution to (4.3) and (4.4) is constructed by means of a meromorphic function $g(w)$ which takes the form

$$g(w) = p \exp[j(w + \alpha_p) \frac{a}{\pi}] \ln 2 \left[\frac{(-1)^p \exp(ju)-1}{w + \alpha_p} \right] \times \prod_{n=1}^{\infty} \left(\frac{1 + \alpha_p / \alpha_n}{1 - w / \alpha_n} \right) \prod_{n=-\infty}^{\infty} \left(\frac{1 - w / \tau_n}{1 + \alpha_p / \tau_n} \right) \quad (4.5)$$

The mode coefficients then are

$$A_q = \frac{R(\alpha_q)}{q [(-1)^q \exp(ju)-1]}, \quad q = 1, 2, 3, \dots \quad (4.6)$$

$$G_q = \frac{\pi g(-\tau_q)}{2a^2 \tau_q}, \quad q = 0, \pm 1, \pm 2, \dots \quad (4.7)$$

These solutions immediately yield the elements of the scattering matrices corresponding to excitation from the (A) or waveguide region. Since the incident wave was the p^{th} mode of unit amplitude, the scattering matrix elements are:

$$S^{AA}(q,p) = A_q, \quad q = 1, 2, 3, \dots \quad (4.8)$$

$$S^{FA}(q,p) = G_q, \quad q = 0, \pm 1, \pm 2, \dots \quad (4.9)$$

where A_q and G_q are given in (4.6) and (4.7), respectively. Solution for each value of p generates the entire scattering matrices, which are implicitly functions of the scan angle θ .

The related scattering matrices corresponding to excitation from the (F) or free-space region are constructed in a similar manner. Assume that the p^{th} free-space mode of unit amplitude is incident upon the array. The electric fields in the waveguide region (A) may be written (m^{th} guide)

$$E_y = \sum_{n=1}^{\infty} A_n \sin\left(\frac{n\pi}{a}(x-na)\right) \exp(-jmu + j\alpha_n z) \quad (4.10)$$

and in the open region (F)

$$E_y = \exp(-j\xi_p x + j\tau_p z) + \sum_{n=-\infty}^{\infty} G_n \exp(-j\xi_n x - j\tau_n z) \quad (4.11)$$

Upon matching E and H fields, the resultant equations may be reduced to

$$\sum_{n=1}^{\infty} n A_n [(-1)^n \exp(ju) - 1] \left(\frac{1}{\alpha_n - \tau_q}\right) - 2 \frac{a^2}{\pi} \tau_p \delta_p^q = 0$$

$$q = 0, \pm 1, \pm 2, \dots \quad (4.12)$$

$$\sum_{n=1}^{\infty} n A_n [(-1)^n \exp(ju) - 1] \left(\frac{1}{\alpha_n + \tau_q}\right) + 2 \frac{a^2}{\pi} \tau_q G_q = 0$$

$$q = 0, \pm 1, \pm 2, \dots \quad (4.13)$$

The solution to this set is constructed from a function

$f(w)$, where

$$f(w) = -2 \frac{a^2}{\pi} \tau_p \exp\left[j(w - \tau_p) \frac{a}{\pi} \ln 2\right] \\ \times \prod_{n=1}^{\infty} \left(\frac{1 - \tau_p/\alpha_n}{1 - w/\alpha_n} \right) \prod_{\substack{n=-\infty \\ n \neq p}}^{\infty} \left(\frac{1 - w/\tau_n}{1 - \tau_p/\tau_n} \right) \quad (4.14)$$

The mode coefficients and hence scattering matrix elements are then

$$A_q = S^{AF}(q,p) = \frac{R_f(\alpha_q)}{q[(-1)^q \exp(ju) - 1]}, \quad q = 1, 2, 3, \dots \quad (4.15)$$

$$G_q = S^{FF}(q,p) = \frac{\pi f(-\tau_q)}{2a^2 \tau}, \quad q = \pm 1, \pm 2, \dots \quad (4.16)$$

The properties of the thin-wall array for each scan angle θ are completely described by the four scattering matrices S^{AA} , S^{AF} , S^{FA} , and S^{FF} . The dominant mode reflection coefficient, which is equal to $S^{AA}(1,1)$, as a function of scan angle is depicted in Figure 4.3 for three values of waveguide width a . The break points in the reflection coefficient curves occur when a second space mode changes from evanescent to propagating.

Thick-wall Array

The model for the thick-wall array for H-plane scan used by Galindo and Wu, and to be used here, is a set of thick, perfectly

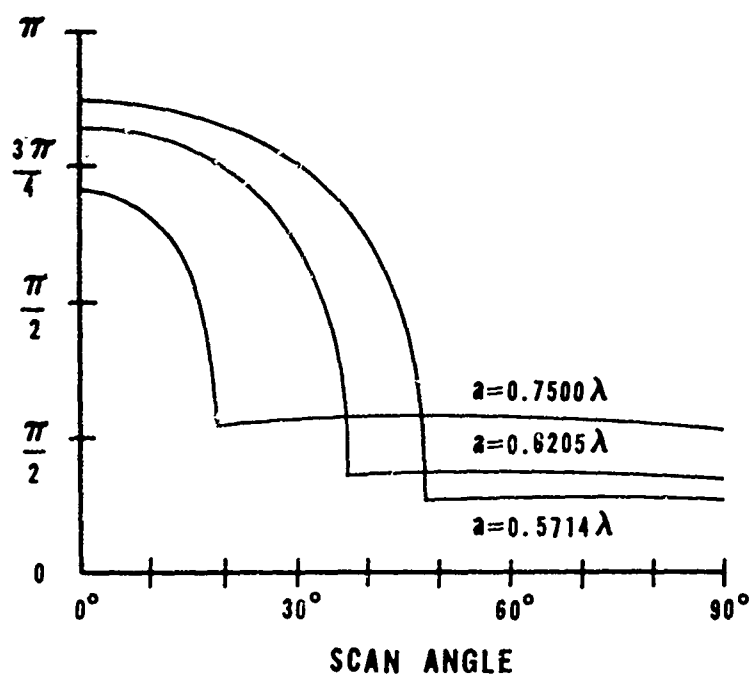
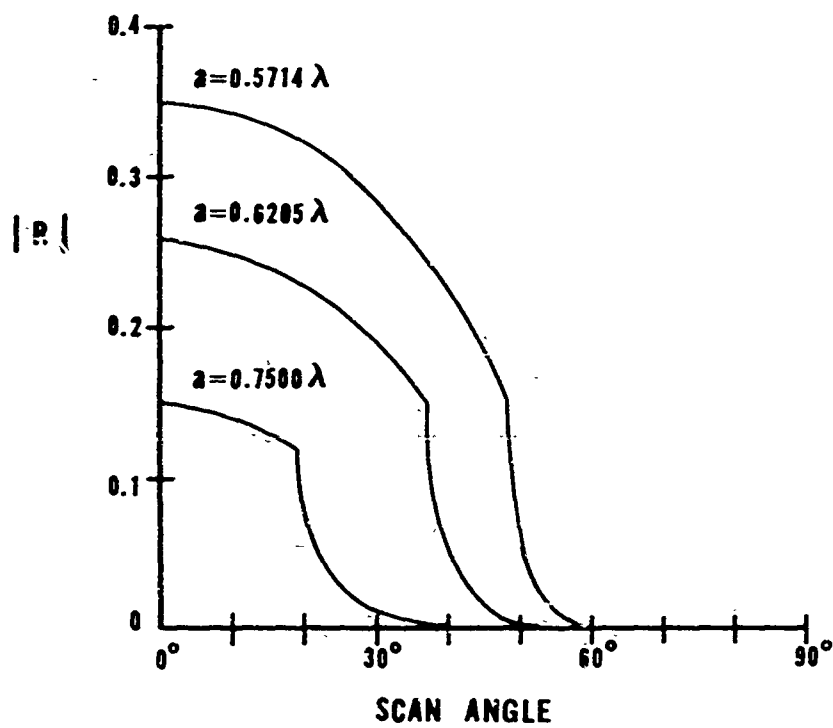


Figure 4.3 Thin-wall array reflection coefficient

conducting, parallel plates, as shown in Figure 4.4. The spaces between the plates may be considered to be parallel plate waveguides, each guide excited from the region $z < 0$ by a TE_{p0} mode. The amplitude of excitation is uniform in each guide, and the phase progresses from guide to guide to scan the main beam of the radiation pattern. The fields in the open (F) region admit a modal expansion of the form (4.2) because of the periodicity of the structure and the excitation.

Despite the modal expansions for the fields on either side of the interface $z = 0$, matching of the transverse components does not lead to a set of equations of the form solvable by the modified residue-calculus technique. However, the modal nature of the fields in regions (B) and (F) suggests description of the array in terms of generalized scattering matrices. The scattering matrices may be derived via the multiple-reflection, Neumann-series method described in Section II for a suitable auxiliary geometry.

The auxiliary geometry appropriate for the thick-wall array is that of Figure 4.5. The junction at $z = 0$ is precisely that of the thin-wall array. An exact scattering matrix description of that junction was given earlier in this section. Let the scattering matrices for the junction have the subscript 1, i.e., S_1^{AA} , S_1^{AF} , S_1^{FA} , S_1^{FF} . On the other hand, the junction at $z = -\delta$ in each waveguide is precisely the step discontinuity described in Section III. Although the general waveguide step problem cannot be solved exactly, a very accurate truncated scattering matrix description of the junction can be found by the MRCT, as in Table 3.2. Let the scattering matrices

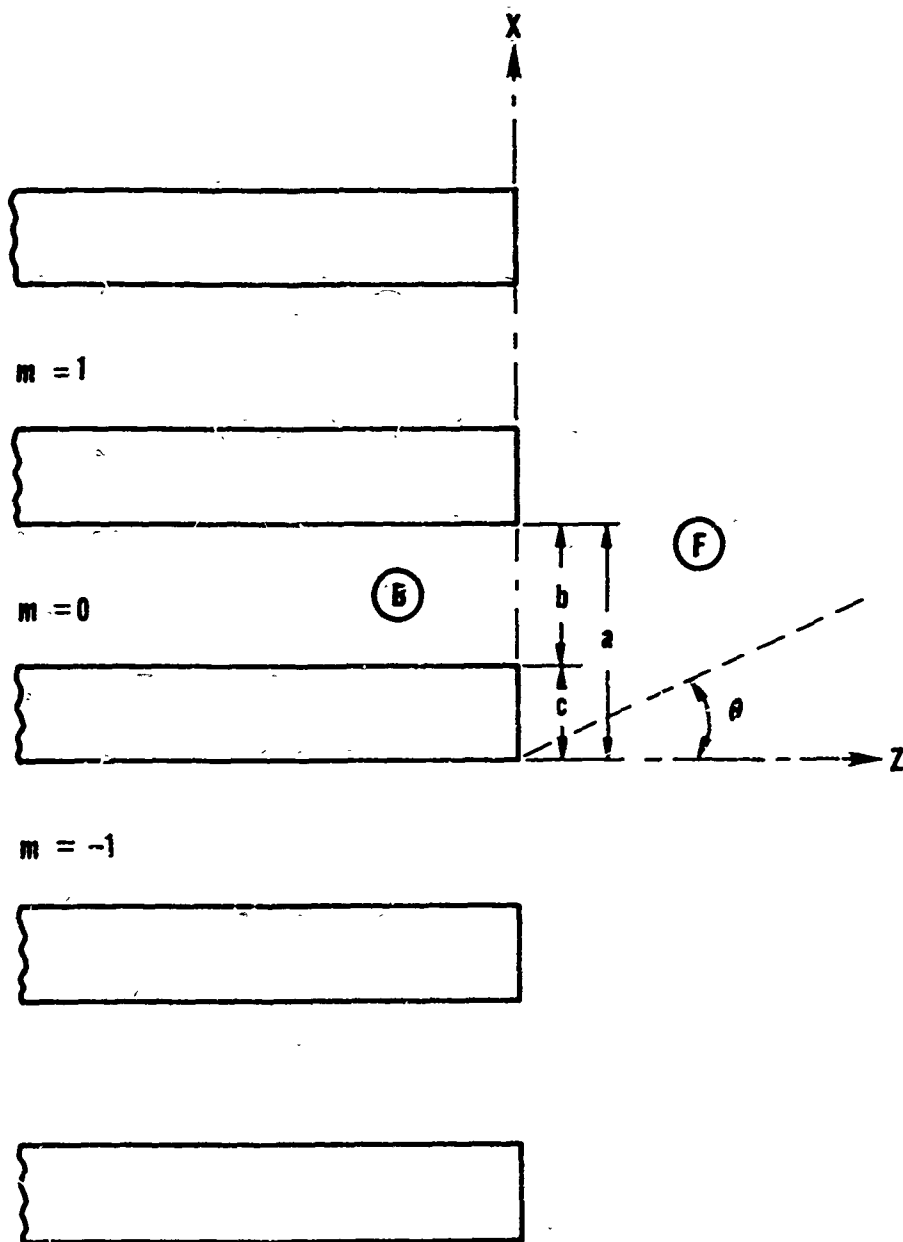


Figure 4.4 Infinite array of thick parallel plates

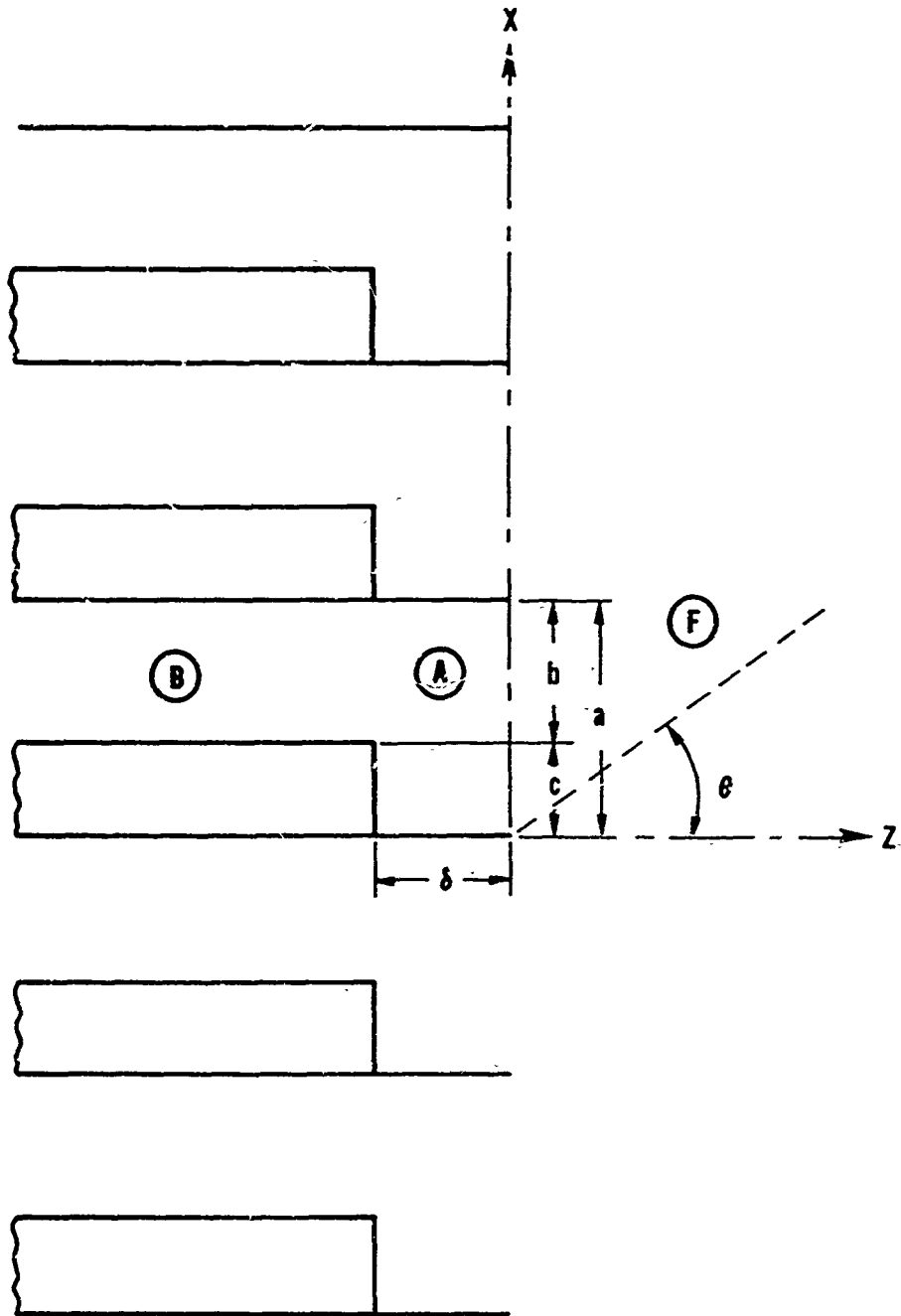


Figure 4.5 Auxiliary geometry for thick-wall array

for this junction carry the subscript 2, i.e., S_2^{AA} , S_2^{AB} , S_2^{BA} , S_2^{BB} . The four scattering matrices for the composite array - S^{BB} , S^{BF} , S^{FB} , S^{FF} - will have no subscript.

Following the multiple-reflection phenomena as depicted in Figure 2.4 and reducing δ to zero yields Neumann series representations for the composite scattering matrices. When summed, these give

$$S^{BB} = S_2^{BB} + S_2^{BA} [I - S_1^{AA} S_2^{AA}]^{-1} S_1^{AA} S_2^{AB} \quad (4.17)$$

$$S^{FB} = S_1^{FA} [I - S_2^{AA} S_1^{AA}]^{-1} S_2^{AB} \quad (4.18)$$

$$S^{BF} = S_2^{BA} [I - S_1^{AA} S_2^{AA}]^{-1} S_1^{AF} \quad (4.19)$$

$$S^{FF} = S_1^{FF} + S_1^{FA} [I - S_2^{AA} S_1^{AA}]^{-1} S_2^{AA} S_1^{AF} \quad (4.20)$$

It must be noted that each scattering matrix with subscript 1 is an implicit function of scan angle, so that the composite scattering matrices also are dependent upon angle.

Because the matrix inversion must be performed numerically it is important to truncate the scattering matrices at the smallest size which yields suitably accurate results. Since the scattering matrix elements must also be computed, keeping the truncated matrices as small as possible also reduces computation time. Just what constitutes "suitably accurate" is a matter of judgment in each case, but numerical results of this section give an indication of variation of dominant mode reflection coefficient for matrix sizes of 1x1, 3x3, and 5x5.

One particular advantage of formulating the thick-wall array in terms of the scattering matrix equations (4.17-20) is that when the wall thickness c reduces to zero, the resultant scattering matrices reduce to exactly the thin-wall scattering matrices. This result occurs because for the case $c=0$, the scattering matrix description of junction 2 yields

$$S_2^{AA} = S_2^{BB} = 0 \quad (4.21)$$

$$S_2^{BA} = S_2^{AB} = I \quad (4.22)$$

Substitution of these values into (4.17-20) reduce the equations to simply the corresponding thin-wall scattering matrices.

Numerical Results

The scattering matrix methods just described were applied to a variety of cases for the thick-wall array. Many of the choices of wall thickness and guide width were made to coincide with those given by Galindo and Wu [1966] to permit comparison of results. In each case, dimensions were chosen to allow only one propagating mode in each waveguide.

In each comparison case, the scattering matrix method gave numerical results for magnitude and phase of the reflection coefficient versus scan angle which were indistinguishable from the results given graphically by Galindo and Wu. By way of further comparison, though, the method of Galindo and Wu was considerably more complicated. For each choice of width, thickness, and scan angle, the appropriate

integral equation was approximately solved by Galerkin's method, and involved solution of a 30×30 set of linear equations. Then a variational correction was applied to obtain the reflection coefficient. On the other hand, the scattering matrix method required solution of two auxiliary problems first by quite elementary means, and then simple combination in the form of equations (4.17-20). Each combination involved the numerical inversion of a 5×5 matrix. Since the solution to the thin-wall array problem is common to all thick-wall arrays for the same width a , and since the solution of each step width is valid for all scan angles, the number of calculations for many related cases is considerably reduced.

The results of computations for one choice of spacing ($a = 0.62\lambda$) and four wall thickness from $c/a = 0$ to $c/a = 0.12$ are summarized in Tables 4.1-4. The reflection coefficients for the thin-wall array (Table 4.1) are based upon the exact solution. In each of the other three cases, approximate results for three sizes of truncated matrices are given. The reflection coefficients found by the 5×5 scattering matrix inversion agrees exactly with the values found by Galindo and Wu, and will be considered to be the "correct" value. The results are also depicted graphically in Figure 4.6.

It is significant to compare the value obtained from the 1×1 matrix with the correct value. Particularly for small scan angles, the 1×1 value is very close to the correct value, often well within one per cent in magnitude and five degrees in phase. Since a 1×1 matrix is simply a complex number, the computation of the reflection coefficient is almost trivial. It is particularly important to

TABLE 4.1

Reflection Coefficient vs. Scan Angle for Thin-Wall

Phased Array ($a/\lambda = 0.6205$)

Scan Angle	Reflection Coefficient (Magnitude, Angle)
0°	(0.2561, 147.5°)
10°	(0.2490, 144.5°)
20°	(0.2268, 133.9°)
30°	(0.1878, 109.3°)
40°	(0.0525, 32.0°)
50°	(0.0021, 32.4°)
60°	(0.0050, 32.4°)
70°	(0.0298, 32.1°)
80°	(0.0745, 31.8°)
90°	(0.1438, 31.7°)

TABLE 4.2

Reflection Coefficient vs. Scan Angle for Thick-Wall Phased Array

$$(a/\lambda = 0.6205, c/a = 0.02)$$

Scan Angle	Reflection Coefficient (Magnitude, Angle)		
	1x1 Matrix	3x3 Matrix	5x5 Matrix
0°	(0.2730, 149.7°)	(0.2740, 148.6°)	(0.2743, 148.0°)
10°	(0.2656, 146.8°)	(0.2665, 145.8°)	(0.2667, 145.2°)
20°	(0.2419, 137.2°)	(0.2427, 136.3°)	(0.2428, 135.7°)
30°	(0.1974, 114.9°)	(0.1978, 114.0°)	(0.1977, 113.4°)
40°	(0.0395, 51.2°)	(0.0393, 49.8°)	(0.0390, 48.9°)
50°	(0.0133, 167.7°)	(0.0182, 168.6°)	(0.0182, 169.3°)
60°	(0.0164, 160.6°)	(0.0162, 161.6°)	(0.0162, 162.4°)
70°	(0.0195, 73.5°)	(0.0192, 72.1°)	(0.0188, 71.3°)
80°	(0.0608, 44.3°)	(0.0608, 43.2°)	(0.0606, 42.4°)
90°	(0.1295, 37.8°)	(0.1298, 36.8°)	(0.1297, 36.1°)

TABLE 4.3

Reflection Coefficient vs. Scan Angle for Thick-Wall Phased Array

 $(a/\lambda = 0.6205, c/a = 0.063)$

Scan Angle	Reflection Coefficient (Magnitude, Angle)		
	1x1 Matrix	3x3 Matrix	5x5 Matrix
0°	(0.3225, 153.3°)	(0.3239, 150.0°)	(0.3240, 148.3°)
10°	(0.3149, 151.0°)	(0.3159, 147.8°)	(0.3156, 146.1°)
20°	(0.2900, 143.4°)	(0.2897, 140.4°)	(0.2884, 138.7°)
30°	(0.2381, 126.4°)	(0.2350, 123.5°)	(0.2317, 121.9°)
40°	(0.0571, 119.6°)	(0.0506, 121.1°)	(0.0463, 123.1°)
50°	(0.0728, 163.0°)	(0.0726, 166.3°)	(0.0725, 168.4°)
60°	(0.0711, 161.2°)	(0.0705, 164.6°)	(0.0703, 166.8°)
70°	(0.0597, 141.8°)	(0.0560, 145.4°)	(0.0538, 148.4°)
80°	(0.0629, 99.1°)	(0.0553, 97.0°)	(0.0500, 96.2°)
90°	(0.1121, 65.0°)	(0.1059, 59.3°)	(0.1009, 55.6°)

TABLE 4.4

Reflection Coefficient vs. Scan Angle for Thick-Wall Phased Array

 $(a/\lambda = 0.6205, c/a = 0.12)$

Scan Angle	Reflection Coefficient (Magnitude, Angle)		
	1x1 Matrix	3x3 Matrix	5x5 Matrix
0°	(0.4261, 158.2°)	(0.4259, 153.3°)	(0.4251, 151.4°)
10°	(0.4193, 156.6°)	(0.4175, 151.9°)	(0.4157, 150.0°)
20°	(0.3961, 151.5°)	(0.3894, 147.2°)	(0.3842, 145.5°)
30°	(0.3429, 140.8°)	(0.3253, 137.3°)	(0.3140, 135.9°)
40°	(0.1711, 146.2°)	(0.1553, 153.6°)	(0.1494, 158.2°)
50°	(0.1902, 160.5°)	(0.1898, 166.7°)	(0.1898, 169.6°)
60°	(0.1888, 159.8°)	(0.1876, 166.1°)	(0.1873, 169.1°)
70°	(0.1783, 153.0°)	(0.1697, 160.1°)	(0.1668, 163.9°)
80°	(0.1667, 139.1°)	(0.1441, 146.0°)	(0.1349, 150.9°)
90°	(0.1719, 115.9°)	(0.1306, 116.3°)	(0.1097, 118.7°)

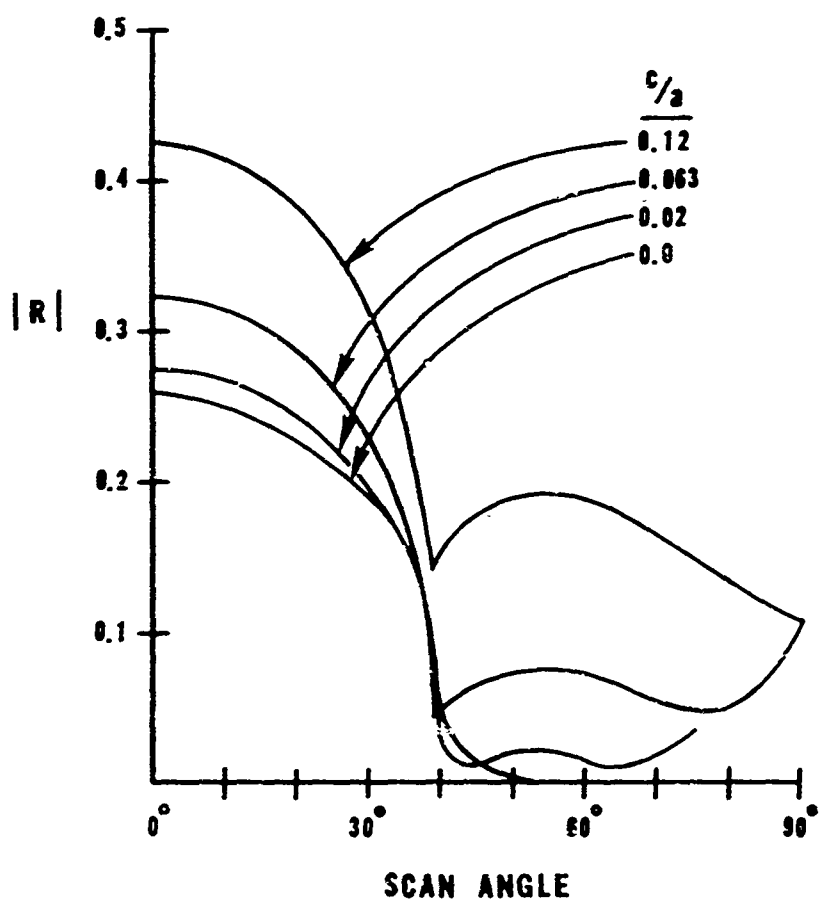


Figure 4.6 Reflection coefficients for thick-wall phased array

notice that simple exact reflection and transmission coefficients for the thin-wall array may be combined with reflection and transmission coefficients for a waveguide step discontinuity (found by the MRCT or even from graphical results, e.g. Marcuvitz [1951]) to yield an excellent approximate result for the thick-wall array. The simplified expression for the array reflection coefficient may be written

$$R = R_2^{BB} + \frac{T_2^{BA} R_1^{AA} T_2^{AB}}{1 - R_2^{AA} R_1^{AA}} \quad (4.23)$$

where

$$R_1^{AA} = S_1^{AA}(1,1)$$

$$R_2^{AA} = S_2^{AA}(1,1)$$

$$R_2^{BB} = S_2^{BB}(1,1)$$

$$T_2^{AB} = S_2^{AB}(1,1)$$

$$T_2^{BA} = S_2^{BA}(1,1)$$

Although the array of Figure 4.4 is shown without dielectric filling in region (B), the solution for dielectric filling proceeds exactly as previously described. The corresponding dielectric-filled step discontinuity is used as part of the auxiliary geometry.

The mode coefficients for the field reflected back into (B) are the elements of the first column of the scattering matrix S^{BB} . The field at the aperture may be readily computed from the modal expansion at $z = 0$, $c \leq x \leq a$. Figure 4.7 illustrates the magnitude of the aperture field for the array at four angles of scan. The array

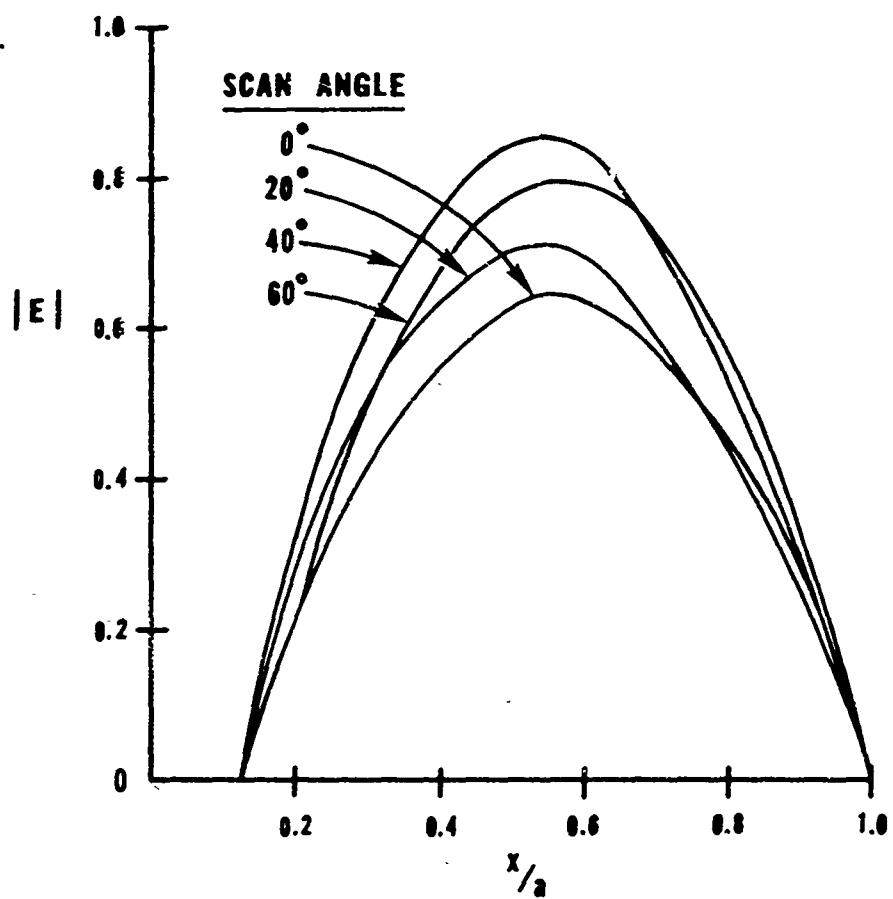


Figure 4.7 Aperture field for thick-wall array

dimensions are $a = 0.62\lambda$, $c/a = 0.12$.

The method described for the solution for the thick-wall array is the first combined application of the MRCT and the generalized scattering matrix method. The principal advantage of the combined technique is that a geometry of some difficulty is reduced to two geometries about which a great deal is known. It uses to advantage the exact solution of the thin-wall array as well as approximate solution to a well known waveguide discontinuity problem. The rapidly convergent numerical technique for such a combined geometry may be quite useful for a number of other problems which can be reduced to two or more auxiliary problems solvable by conventional methods or by the MRCT. Solutions for a class of such problems, specifically diffracting surfaces and gratings, are discussed in the next section.

V. DIFFRACTING SURFACES AND GRATINGS

The modified residue-calculus technique and the scattering matrix multiple-reflection procedure can be combined to attack a wide variety of interesting problems, such as diffraction by a finite circular cylinder, scattering from a semi-infinite cylinder of rectangular cross section, and reflection at a dielectric step discontinuity, to cite only a few. Another class of problems consists of periodic diffraction surfaces and gratings. Since gratings are finding current applications, for example in resonators for lasers operating at suboptical frequencies, alternative simple methods for accurately finding reflection and transmission properties of gratings and surfaces can be quite useful.

The general form of the periodic diffracting surface treated in this section is shown in Figure 5.1. The geometry is essentially that of the array of thick plates with a recessed dielectric filling. Because the scattering matrix representation of the array of thick plates is readily obtainable by the techniques of Section IV and because the scattering matrices for the junction between (B) and (B') may be found exactly, the combined geometry is most suitable for description in terms of the multiple reflection phenomena.

An application of scattering matrix methods to diffracting surfaces has been made by Tseng [1967], who discussed in detail diffraction and surface wave propagation on infinite periodic corrugated surfaces. Although the corrugating fins were of zero thickness in Tseng's problem, the most general unit cell included multiple corrugations of various depths.

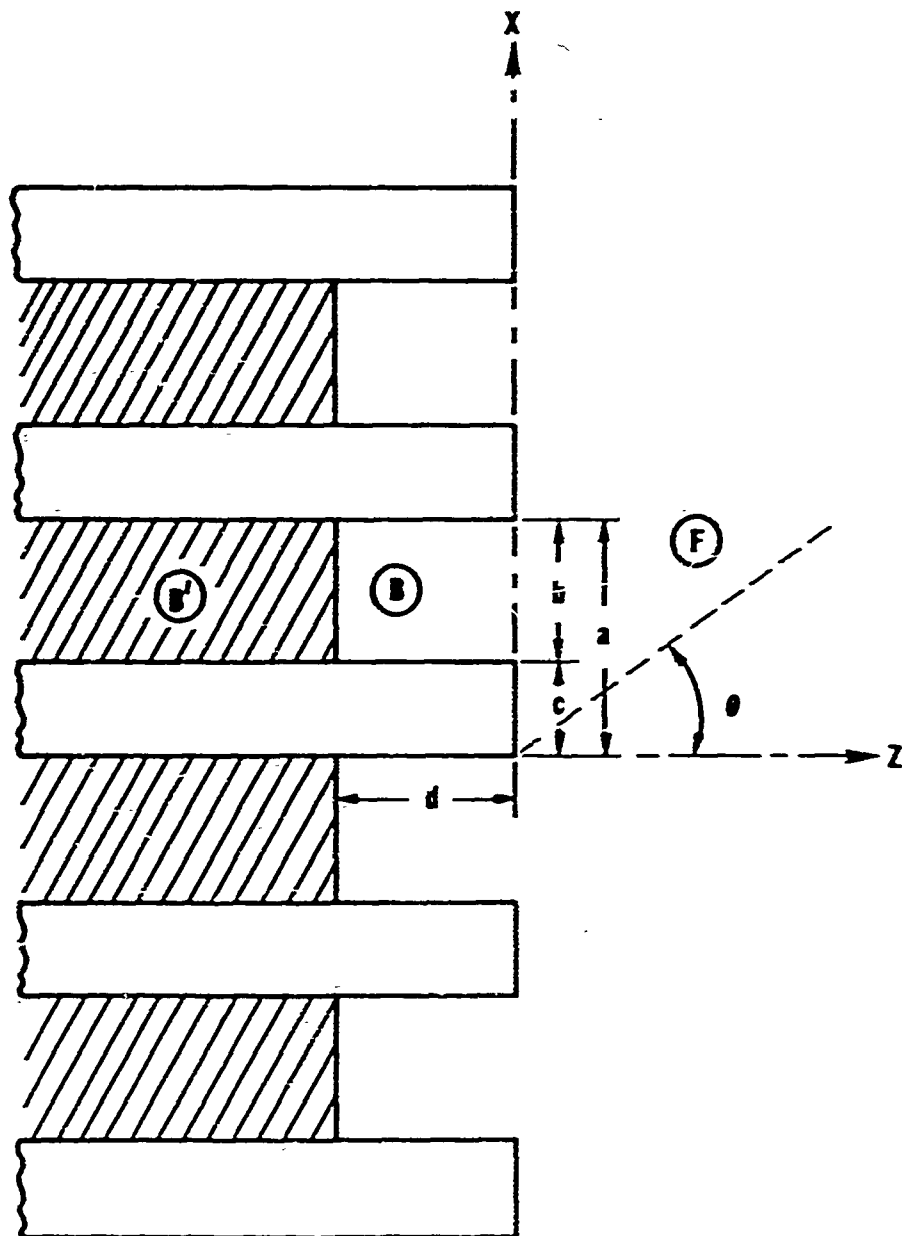


Figure 5.1 Infinite periodic diffracting surface

To avoid repetition of the work of Tseng, only the formal analysis for a few selected geometries is discussed in this section, primarily to indicate the extension of the MRCT and scattering matrix procedure to cases other than the waveguide discontinuities and array problems treated previously.

Analysis

Let the junction at $z = 0$ in Figure 5.1 be designated by the subscript 1, so that the scattering matrices for that junction, found in Section IV, are S_1^{BB} , S_1^{BF} , S_1^{FB} , and S_1^{FF} . The modal expansion in the open region (F) is the same as described in Section IV. Further, let the junction between (B) and (B') be denoted by subscript 2. The scattering matrix of interest at that junction is S_2^{BB} . If the dielectric in (B') has relative dielectric constant ϵ_b , the scattering matrix elements are given by

$$S_2^{BB}(n,m) = \delta_n^m \left(\frac{\beta_n - \bar{\beta}_n}{\beta_n + \bar{\beta}_n} \right) \quad (5.1)$$

where

$$\beta_n = \sqrt{k_o^2 - (n\pi/b)^2}$$

$$\bar{\beta}_n = \sqrt{\epsilon_b k_o^2 - (n\pi/b)^2}$$

are the propagation constants for the n^{th} mode in (B) and (B'), respectively. Limiting cases of perfect electric and magnetic conductors in (B') yields

$$S_2^{BB} = -I \quad (5.2)$$

for electric wall at $z=-d$, and

$$S_2^{BB} = + I$$

for the magnetic wall. The surface with electric wall at $z=-d$ is shown in Figure 5.2.

An essential part of the diffracting surface is the recession distance d . Propagation of the modes in guide (B) is represented by the propagation matrix Γ , where

$$\Gamma(n,m) = \delta_n^m \exp(-j\beta_n d) \quad (5.4)$$

For example, propagation from $z = 0$ to $z=-d$, reflection at junction 2, and propagation back from $z=-d$ to $z = 0$ is represented by $\Gamma S_2^{BB} \Gamma$. Since the high-order modes are evanescent, the effect of the propagation matrix Γ is to suitably weight them. The result is that truncation at small matrix sizes (5x5, say) causes negligible error.

The multiple reflections for a wave incident from region (F) yield the following expression for the composite scattering matrix S^{FF}

$$\begin{aligned} S^{FF} &= S_1^{FF} + S_1^{FB} \Gamma S_2^{BB} \Gamma S_1^{BF} \\ &+ S_1^{FB} \Gamma S_2^{BB} \Gamma S_1^{BB} \Gamma S_2^{BB} \Gamma S_1^{BF} \\ &+ S_1^{FB} \Gamma S_2^{BB} \Gamma (S_1^{BB} \Gamma S_2^{BB} \Gamma)^2 S_1^{BF} + \dots \\ &= S_1^{FF} + S_1^{FB} \Gamma S_2^{BB} \Gamma (I - S_1^{BB} \Gamma S_2^{BB} \Gamma)^{-1} S_1^{BF} \end{aligned} \quad (5.5)$$

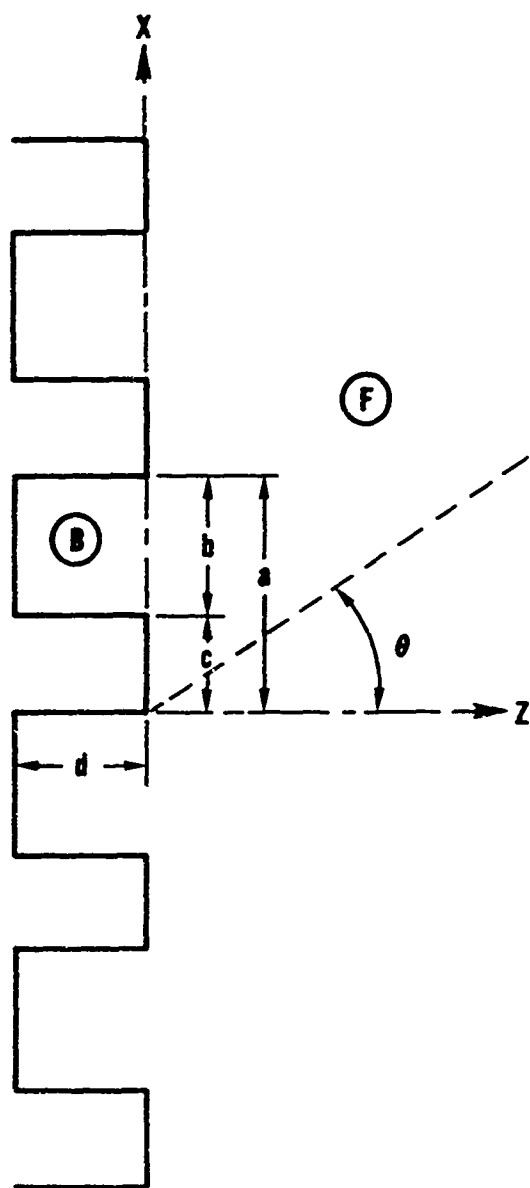


Figure 5.2 Metallic modulated diffracting surface

The scattering matrix S^{FF} is of course a function of the incident angle θ , because every scattering matrix with subscript 1 is an implicit function of angle.

For the surface with dielectric filling, the transmission into the dielectric region may also be found by the scattering matrix method, so that

$$S^{B'F} = S_2^{B'B} \Gamma (I - S_1^{BB} \Gamma S_2^{BB} \Gamma)^{-1} S_1^{BF} \quad (5.6)$$

An alternative interpretation of the geometry of Figure 5.1 is a phased array with recessed dielectric filling, so that reflection coefficients for periodic excitation from region (B') may also be found by the generalized scattering matrix method.

Strip grating. The diffraction grating formed by an infinite set of thin parallel strips as shown in Figure 5.3 may also be treated by the multiple-reflection scattering matrix procedure. As with the waveguide diaphragm of Section III, the grating may be reduced to two solvable auxiliary geometries by considering symmetric and antisymmetric excitation on either side of the grating. Suppose the grating is excited equally and symmetrically from both sides. For this excitation, the transverse magnetic field H_x in the apertures of the gratings is exactly zero, so that a magnetic wall may be placed in each aperture without effect. As viewed from region (F), the structure for symmetric excitation becomes alternate magnetic and electric strips, which is a limiting case of Figure 5.1 as the dielectric in (B') becomes a magnetic wall and distance d reduces to zero. For equal but antisymmetric excitation, the electric fields

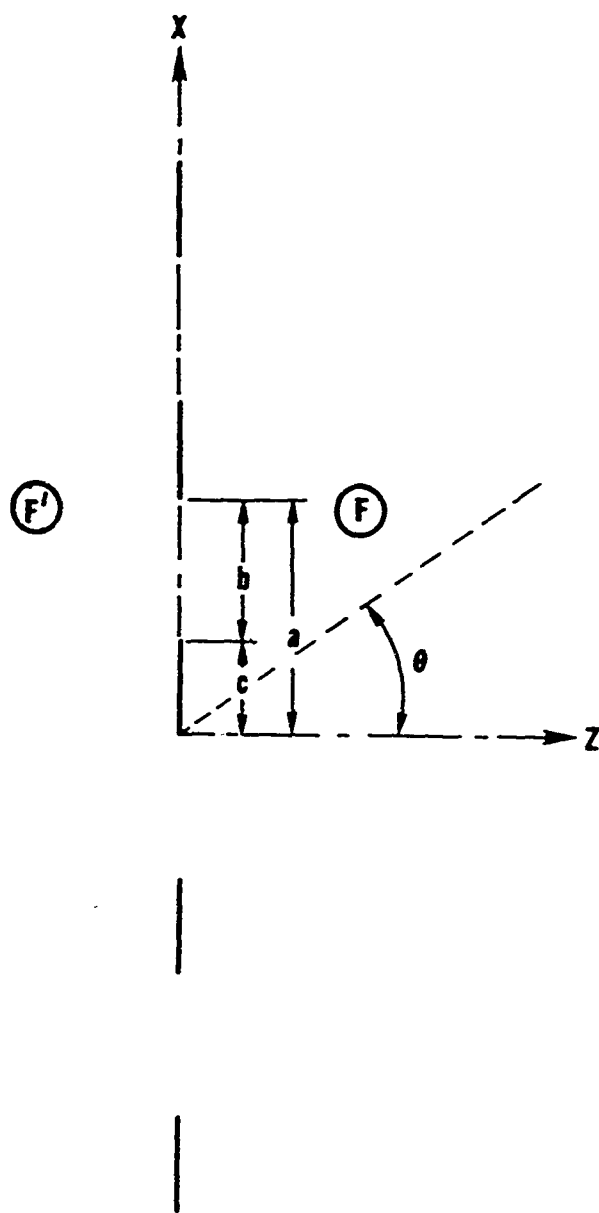


Figure 5.3 Infinite grating of thin strips

cancel exactly in the aperture and the grating may be replaced by a perfect electric conducting wall.

The solution for the magnetic-electric strip grating may be obtained from equation (5.5). However, the scattering matrix $S_2^{BB} = I$ (as in (5.3)) and for $d=0$, the propagation matrix also becomes $\Gamma=I$. In that instance, then,

$$S_s^{FF} = S_1^{FF} (I - S_1^{BB})^{-1} S_1^{BF} \quad (5.7)$$

where the subscript s denotes symmetric excitation. By inspection, the scattering matrix for the electric wall is

$$S_a^{FF} = -I \quad (5.8)$$

where the subscript a denotes antisymmetric excitation.

For simultaneous symmetric and antisymmetric excitation, the incident waves from (E') cancel and the waves from (F) add. As a result, the composite scattering matrix for the strip grating may be written

$$\begin{aligned} S^{FF} &= \frac{1}{2}(S_s^{FF} + S_a^{FF}) \\ &= \frac{1}{2}(S_s^{FF} - I) \end{aligned} \quad (5.9)$$

Numerical results for selected diffracting surfaces were computed to test the multiple-reflection method. In all of the test cases, the reflection coefficients were consistent with known power requirements, even with more than one space mode propagating. Reflection

coefficients for two cases are given in Table 5.1. The geometry is that of Figure 5.2. For both cases, the width is $a = 0.75\lambda$ and depth $d = 0.5\lambda$. Case 1 has $c=0$ and Case 2 has $c=0.3a$. Case 1 is the geometry of Tseng [1967].

TABLE 5.1
Reflection Coefficient for Diffracting Surface
($a = 0.75\lambda$, $d = 0.5\lambda$)

Incident Angle θ	Reflection Coefficient	
	Case 1. $c/a = 0$	Case 2. $c/a = 0.3$
0°	$0.3845 - j0.9231$	$0.0177 + j0.9998$
15°	$0.1586 - j0.9873$	$0.0732 + j0.9981$
30°	$-0.2293 - j0.3921$	$0.0209 + j0.6055$
45°	$-0.3139 - j0.0413$	$-0.2406 + j0.4956$

Although the discussion of diffraction surfaces in this section is rather brief and restricted to a few basic geometries, the combined MRCT and scattering matrix procedures may be applied to a wide class of surface and grating problems. Many variants on the geometry of Figure 5.1 are possible, including geometries in which reflections at more than two junctions are considered.

VI. CONCLUSIONS

The analytical methods described in this thesis provide a very accurate and very rapid numerical means for solving a class of boundary value problems related to basic Wiener-Hopf geometries. As compared to some variational or integral-equation techniques for solving the same types of problems, the MRCT and the scattering matrix method, or both together, yield the most often required information, i.e., scattering coefficients, in a very simple form, without need for the iterative procedures, numerical integrations, or large order matrix inversions which often are time consuming and potentially inaccurate from a computational standpoint. A particular advantage of the methods described here is that in a modified Wiener-Hopf geometry, a great deal of information already known about the related auxiliary geometry is utilized in the more complicated problem. For example, independent solutions of the waveguide step discontinuity and of the array of thin plates may readily be combined to solve a much more difficult problem of great practical interest, namely the thick-wall phased array.

One additional property of the MRCT is particularly significant. The MRCT automatically satisfies the edge condition of the problem being solved, even when the edge condition differs from that of the auxiliary geometry, because *a priori* information about the edge condition is incorporated into the construction of the required meromorphic function. In contrast, satisfaction of the edge condition in solution of a doubly infinite set of equations by

truncation is strongly dependent upon the truncation procedure (Mittra [1963]).

Although a variety of waveguide discontinuities were solved by the MRCT, combination with the scattering matrix procedure permits solution of such problems as thick diaphragms, trifurcations (Pace [1964]), multiple diaphragms, and rectangular posts in waveguides. Also, the MRCT can be extended to circular cylindrical geometries, so that a variety of corresponding discontinuities in circular waveguides may be solved.

The applicability of the analytical methods of this thesis to a wide variety of problems in both open and closed regions will permit numerical solutions in a convenient form for many problems of current interest.

REFERENCES

- Berz, F. [1951], Reflection and refraction of microwaves at a set of parallel metallic plates. *Proc. IEE (London)*. 98, III: 47-55.
- Carlson, J. F., and Heins, A. E. [1947], The reflection of an electromagnetic wave by an infinite set of plates. *Quart. Appl. Math.* 4:313-329 and 5:82-88.
- Collin, R. E. [1960], *Field Theory of Guided Waves*. New York: McGraw-Hill.
- Collin, R. E. [1966], *Foundations for Microwave Engineering*. New York: McGraw-Hill.
- Galindo, V., and Wu, C. P. [1966], Numerical solutions for an infinite phased array of rectangular waveguides with thick walls. *IEEE Trans. on Antennas and Propagation*. AP-14, No. 2:149-158.
- Lee, S. W. [1967], Radiation from an infinite array of parallel-plate waveguides with thick walls. *IEEE Trans. Microwave Theory and Techniques*. MTT-15, No. 6:364-371.
- Marcuvitz, N. [1951], *Waveguide Handbook*. MIT Rad. Lab. Series, 10. New York: McGraw-Hill.
- Mitra, R. [1963], Relative convergence of the solution of a doubly infinite set of equations. *J. Res. NBS*. 67D:245-254.
- Mitra, R., Lee, S. W., and VanBlaricum, G. F. [1968], A modified residue calculus technique. Antenna Laboratory, University of Illinois, Report 68-1.
- Mitra, R., and Pace, J. [1963], A new technique for solving a class of boundary value problems. Antenna Laboratory, University of Illinois, Report 72.
- Noble, B. [1958], *Methods Based on the Wiener-Hopf Technique*. London: Pergamon Press.
- Pace, J. [1964], The generalized scattering matrix analysis of waveguide discontinuity problems. Antenna Laboratory, University of Illinois, Report 1.
- Seshu, S., and Balabanian, N. [1959], *Linear Network Analysis*. New York: Wiley.
- Tseng, D. Y. [1967], Guiding and scattering of electromagnetic fields by corrugated structures. Department of Electrophysics, Polytechnic Institute of Brooklyn, Scientific Report PIBMRI-1371-67.

- Whitehead, E. A. N. [1951], The theory of parallel plate media for microwave lenses. *Proc. IEE (London)*. 98, III:133-140.
- Wiener, N., and Hopf, E. [1931], Über eine Klasse singulärer Integralgleichungen. *S. B. Preuss. Akad. Wiss.* 696-706.
- Wu, C. P., and Galindo, V. [1966], Properties of a phased array of rectangular guides with thin walls. *IEEE Trans. on Antennas and Propagation*. AP-14, No. 2:163-173.

Unclassified

Security Classification

DOCUMENT CONTROL DATA - R&D		
<i>(Security classification of title, body of abstract and indexing annotation must be entered when the overall report is classified)</i>		
1. ORIGINATING ACTIVITY (Corporate author) University of Illinois Urbana, Illinois 61801	2A. REPORT SECURITY CLASSIFICATION Unclassified	2B. GROUP
3. REPORT TITLE SOME ANALYTICAL METHODS FOR SOLVING A CLASS OF BOUNDARY VALUE PROBLEMS		
4. DESCRIPTIVE NOTES (Type of report and inclusive dates) scientific. interim.		
5. AUTHOR(S) (Last name, first name, initial) G. F. VanBlaricum, Jr. R. Mittra		
6. REPORT DATE June 1966	7A. TOTAL NO. OF PAGES 95	7B. NO. OF REFS 17
8A. CONTRACT OR GRANT NO. AF 19(628)-3819	8B. ORIGINATOR'S REPORT NUMBER(S) Technical Report No. 16 Antenna Laboratory No. 68-3	
9. PROJECT AND TASK NO. C Z	9A. OTHER REPORT NO(S) (Any other numbers that may be assigned this report)	
10. AVAILABILITY/LIMITATION NOTES: 1 - Distribution of this document is unlimited. It may be released to the Clearinghouse, Department of Commerce, for sale to the general public.		
11. SUPPLEMENTARY NOTES TECH, OTHER	12. SPONSORING MILITARY ACTIVITY Air Force Cambridge Research Laboratories (CRD) L. G. Hanscom Field Bedford, Massachusetts 01730	
13. ABSTRACT —A variety of boundary problems, related to basic Wiener-Hopf geometries but of more practical interest, has been solved by a modified residue-calculus technique (MRCT), by the generalized scattering matrix technique, or by a combination of the two methods. The MRCT solution is given in a form convenient for computation, not involving numerical integration or solution of large order matrix equations. In addition, the MRCT automatically guarantees satisfaction of the edge condition and includes built-in tests on the convergence of the solution. An additional group of modified Wiener-Hopf geometries in which modal expansions are possible are solved by a combination of the MRCT and the generalized scattering matrix procedure. The analytical methods described in this report are applicable to waveguide discontinuities, including steps, bifurcations, and diaphragms, in both rectangular and circular waveguides; to phased arrays of dielectric-filled waveguides with thick walls; to a variety of diffraction surfaces and gratings; and to many other modified Wiener-Hopf geometries.		

DD FORM 1473
1 JAN 64

Unclassified

Security Classification

34. KEY WORDS	LINK A		LINK B		LINK C	
	ROLE	WT	ROLE	WT	ROLE	WT
Modified Residue-Calculus Method						
Waveguide Discontinuity						
Waveguide Phased Arrays						
Wiener-Hopf Technique						
Diffraction						
Generalized Scattering Matrix						

INSTRUCTIONS

1. **ORIGINATING ACTIVITY:** Enter the name and address of the contractor, subcontractor, grantee, Department of Defense activity or other organization (corporate number) issuing the report.

2a. **REPORT SECURITY CLASSIFICATION:** Enter the overall security classification of the report. Indicate whether "Restricted Data" is included. Marking is to be in accordance with appropriate security regulations.

2b. **GROUP:** Automatic downgrading is specified in DoD Directive 5300.10 and Armed Forces Industrial Manual. Enter the group number. Also, when applicable, show that optional markings have been used for Group 3 and Group 4 as authorized.

3. **REPORT TITLE:** Enter the complete report title in all capital letters. Titles in all cases should be unclassified. If a meaningful title cannot be selected without classification, show title classification in all capitals in parenthesis immediately following the title.

4. **DESCRIPTIVE NOTES:** If appropriate, enter the type of report, e.g., interim, progress, summary, annual, or final. Give the inclusive dates when a specific reporting period is covered.

5. **AUTHOR(S):** Enter the name(s) of author(s) as shown on or in the report. Enter last name, first name, middle initial. If military, show rank and branch of service. The name of the principal author is an absolute minimum requirement.

6. **REPORT DATE:** Enter the date of the report as day, month, year, or month, year. If more than one date appears on the report, use date of publication.

7a. **TOTAL NUMBER OF PAGES:** The total page count should follow normal pagination procedures, i.e., enter the number of pages containing information.

7b. **NUMBER OF REFERENCES:** Enter the total number of references cited in the report.

8a. **CONTRACT OR GRANT NUMBER:** If appropriate, enter the applicable number of the contract or grant under which the report was written.

8b, 8c, & 8d. **PROJECT NUMBER:** Enter the appropriate military department identification, such as project number, subproject number, system numbers, task number, etc.

9a. **ORIGINATOR'S REPORT NUMBER(S):** Enter the official report number by which the document will be identified and controlled by the originating activity. This number must be unique to this report.

9b. **OTHER REPORT NUMBER(S):** If the report has been assigned any other report numbers (either by the originator or by the sponsor), also enter this number(s).

10. **AVAILABILITY/LIMITATION NOTICES:** Enter any limitations on further dissemination of the report, other than those imposed by security classification, using standard statements such as:

- (1) "Qualified requesters may obtain copies of this report from DDC."
- (2) "Foreign announcement and dissemination of this report by DDC is not authorized."
- (3) "U. S. Government agencies may obtain copies of this report directly from DDC. Other qualified DDC users shall request through _____."
- (4) "U. S. military agencies may obtain copies of this report directly from DDC. Other qualified users shall request through _____."
- (5) "All distribution of this report is controlled. Qualified DDC users shall request through _____."

If the report has been furnished to the Office of Technical Services, Department of Commerce, for sale to the public, indicate this fact and enter the price, if known.

11. **SUPPLEMENTARY NOTES:** Use for additional explanatory notes.

12. **SPONSORING MILITARY ACTIVITY:** Enter the name of the departmental project office or laboratory sponsoring (paying for) the research and development. Include address.

13. **ABSTRACT:** Enter an abstract giving a brief and factual summary of the document indicative of the report, even though it may also appear elsewhere in the body of the technical report. If additional space is required, a continuation sheet shall be attached.

It is highly desirable that the abstract of classified reports be unclassified. Each paragraph of the abstract shall end with an indication of the military security classification of the information in the paragraph, represented as (TS), (S), (C), or (U).

There is no limitation on the length of the abstract. However, the suggested length is from 150 to 225 words.

14. **KEY WORDS:** Key words are technically meaningful terms or short phrases that characterize a report and may be used as index entries for cataloging the report. Key words must be selected so that no security classification is required. Identifiers, such as equipment model designation, trade name, military project code name, geographic location, may be used as key words but will be followed by an indication of technical context. The assignment of links, rules, and weights is optional.